Geology and lithogeochemistry of hydrothermal mudstones from the upper block near the Duck Pond volcanogenic massive sulfide (VMS) deposit, Newfoundland, Canada: evidence for low-temperature venting into oxygenated mid-Cambrian seawater

Stephen J. Piercey, Gerry Squires & Terry Brace

Mineralium Deposita
International Journal for Geology, Mineralogy and Geochemistry of Mineral Deposits

ISSN 0026-4598

Miner Deposita
DOI 10.1007/s00126-018-0795-3

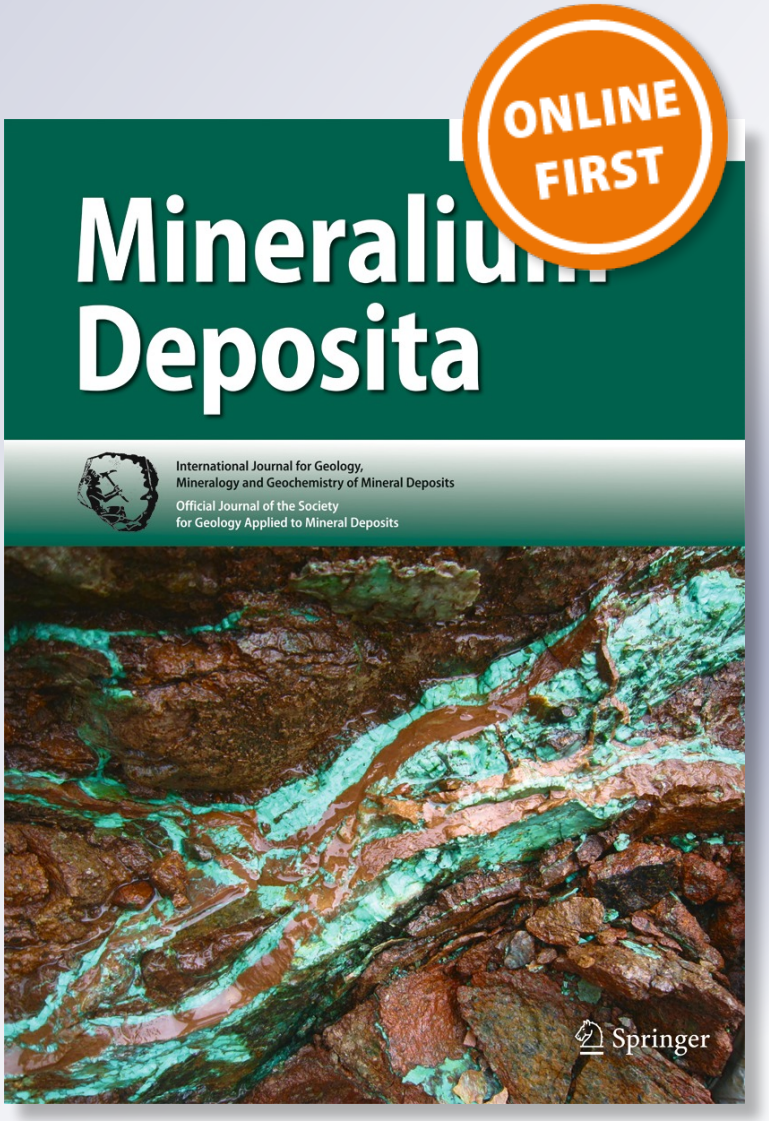

Springer

Mineralium Deposita
https://doi.org/10.1007/s00126-018-0795-3

ARTICLE

Geology and lithogeochemistry of hydrothermal mudstones from the upper block near the Duck Pond volcanogenic massive sulfide (VMS) deposit, Newfoundland, Canada: evidence for low-temperature venting into oxygenated mid-Cambrian seawater

Stephen J. Piercey[1] · Gerry Squires[2] · Terry Brace[3]

Received: 1 March 2017 / Accepted: 31 January 2018

Abstract

Pyrite- and pyrrhotite-rich mudstones are spatially associated with Cambrian (~ 512–509 Ma) volcanogenic massive sulfide (VMS) deposits throughout the Tally Pond group, central Newfoundland, Canada. At the Duck Pond mine, sulfide-rich mudstones are hosted within a weakly mineralized upper block that structurally overlies the deposit but is older (~ 513 versus 509 Ma). The mudstones are laminated, 10–30-cm thick, and pyrite- and pyrrhotite-rich and occur along pillow lava selvages, or in between pillow lavas, rhyolite flows, and volcaniclastic rocks. The mudstones are laterally extensive and proximal to the mudstone host rocks are hydrothermally altered to epidote-quartz-chlorite (basalt host) and sericite-quartz (rhyolite host). Lithogeochemical data for the sulfide-rich mudstones reflect the varying contributions of elements from sedimentary detritus, hydrothermal discharge, and hydrogenous scavenging from middle Cambrian seawater. The mudstones have minor detrital element abundances and significant hydrothermal element enrichments (i.e., elevated Fe_2O_3, S, Pb, Zn, Cu, and Ba concentrations, high Fe/Al ratios). The hydrothermal mudstones are also enriched in oxyanions (i.e., P_2O_5, U, V, Cr, Ni, Co, and Hg), interpreted to have been enriched via oxidative scavenging from seawater by Fe-oxide/oxyhydroxide particles. The mudstones also have REE-Y signatures similar to modern oxygenated seawater with high Y/Ho and negative Ce anomalies (Ce/Ce* = 0.40–0.86; average = 0.58), which correlate with adsorbed oxyanion concentrations. The low Eu/Eu* (1.02–1.86; average = 1.22) in the mudstones suggest that they were deposited from low-temperature (< 250 °C), Fe-rich hydrothermal fluids that likely formed a buoyant plume into an oxygenated water column. The REE-Y-oxyanion signatures suggest that the particles within the hydrothermal plume had sufficient residence time to scavenge oxyanions from seawater and inherit a middle Cambrian seawater signature. The predominant seawater REE-Y-oxyanion signature in the Duck Pond upper block sulfide-rich mudstones suggests that they are distal hydrothermal sedimentary rocks that could have formed up to 10 km from their original vent sources. Correspondingly, to utilize hydrothermal mudstones as vectors to mineralization in the Tally Pond belt, and similar belts globally, it is critical to identify vent-proximal samples that have hydrothermal signatures (i.e., high Fe/Al, base metals, Ba, S), with subdued seawater and adsorption signatures (i.e., chondritic Y/Ho, low P_2O_5, Ni, U, Co, Cr, V, and Hg), indicating minimal residence time in the water column and deposition proximal to the vent.

Editorial handling: K. Kelley

Electronic supplementary material The online version of this article (https://doi.org/10.1007/s00126-018-0795-3) contains supplementary material, which is available to authorized users.

✉ Stephen J. Piercey
spiercey@mun.ca

[1] Department of Earth Sciences, Memorial University of Newfoundland, 300 Prince Philip Drive, St. John's, NL A1B 3X5, Canada

[2] G.C. Squires Geological Consulting, 10 Fair Haven Place, St. John's, NL A1E 4S1, Canada

[3] Mount Pearl, Canada

Introduction

Volcanogenic massive sulfide (VMS) deposits are commonly spatially and temporally associated with fine-grained, Fe-rich hydrothermal sedimentary rocks. Hydrothermal sedimentary rocks have various compositions, including hematite-rich cherty horizons (Kalogeropoulos and Scott 1983; Kalogeropoulos and Scott 1989; Grenne and Slack 2005; Slack et al. 2007, 2009), magnetite-rich iron formation (Peter and Goodfellow 1996; Peter et al. 2003), and sulfide-rich shales/mudstones (Hrischeva and Scott 2007; Hrischeva

Published online: 26 February 2018

et al. 2007; Lode et al. 2015, 2016a, b). These Fe-rich sedimentary horizons are interpreted to be records of ancient Fe-oxide/oxyhydroxide (± sulfide) discharge (i.e., hydrothermal plume material) from seafloor hydrothermal vents (Peter 2003). In the modern and ancient record, hydrothermal discharge resulted in the deposition of Fe-rich particles over considerable distances (up to 10s of kilometers) commonly forming laterally extensive Fe-rich hydrothermal sedimentary rocks that have distinctive changes in texture, mineralogy, and lithogeochemistry with distance from a vent (e.g., Rudnicki 1995; German and Von Damm 2003; Peter 2003; Lode et al. 2015, 2016b).

In the ancient geological record, these laterally extensive hydrothermal sedimentary rocks are potentially important exploration vectors as, in many cases, they reflect the original mineralogical, textural, and lithogeochemical variations that existed on the seafloor. Therefore, by utilizing the mineralogy, textures, and lithogeochemical variations in these ancient hydrothermal sedimentary rocks, it is possible to outline proximity and relative distances from mineralization (Peter and Goodfellow 1996; Peter 2003; Peter et al. 2003; Grenne and Slack 2005). Further, hydrothermal sedimentary rock geochemistry, mineralogy, and isotope signatures can be used to infer ancient ambient ocean oxidation state and hydrothermal plume dynamics in ancient seafloor hydrothermal systems (Peter 2003; Slack et al. 2007).

In this study, we provide an integrated geological and lithogeochemical study of mid-Cambrian sulfide-rich mudstones within a thrust-imbricated panel of bimodal volcanic rocks structurally above the Duck Pond deposit (upper block) that is weakly mineralized, and older (~ 513 Ma) than the ore-hosting mineralized block (~ 509 Ma). While older than the underlying Duck Pond deposit, the hydrothermal mudstones are hosted in a similar stratigraphic package, and are time equivalents, to mineralization-associated mudstones at the Lemarchant VMS deposit ~ 10 km south of the Duck Pond deposit (Lode et al. 2015, 2016a, b). Thus, these hydrothermal mudstones provide an opportunity to evaluate vent-distal hydrothermal sedimentary rocks in the ancient geological record. In this paper, we provide a geological framework for these sulfide-rich mudstones and use their lithogeochemistry to understand the provenance, nature of hydrothermal plume activity, seawater oxidation state, and applications to exploration vectoring within the Duck Pond belt and similar geological environments globally.

Regional geological and metallogenic setting

The Duck Pond VMS deposit is located within the Newfoundland Appalachians, which is divided into four tectonostratigraphic zones, from west to east (Williams 1979; Williams et al. 1988; Hibbard et al. 2006): the Humber, Dunnage, Gander, and Avalon zones (Fig. 1). The Dunnage zone, the central portion of the orogen, commonly called the Central Mobile Belt, represents the vestiges of the Iapetus Ocean, consisting of arc, back-arc, and ophiolitic rocks that formed along the margins of Laurentia (Notre Dame subzone) and Gondwana (Exploits subzone) in the Cambrian to Ordovician (Fig. 1) (Swinden et al. 1989; Swinden 1991; Kean et al. 1995; van Staal and Colman-Sadd 1997; Evans and Kean 2002; Rogers and van Staal 2002; Rogers et al. 2006, 2007; van Staal 2007). The Notre Dame and Exploits subzones were subsequently accreted to the margins of the Laurentian and Gondwanan margins, during the Ordovician Taconic and Penobscot orogenies, respectively, in the Ordovician, and to one another during the Silurian Salinic orogeny (van Staal 2007; Zagorevski et al. 2007a, 2010).

The Dunnage zone is host to most of the VMS deposits in the Appalachian orogen, including the world-class Bathurst Mining Camp, along strike in the New Brunswick Applachians (Goodfellow et al. 2003a), and the past-producing world-class deposits of the Buchans Mining Camp in the southwestern part of the Buchans-Roberts Arm belt (Thurlow 2010; deposits 17–28 on Fig. 1). The Dunnage zone is also host to numerous other producing (e.g., Ming) and past-producing deposits (e.g., Duck Pond, Boundary) (Fig. 1). Volcanogenic massive sulfide deposits are hosted in both the Notre Dame and Exploits subzones (Fig. 1). The deposits north of the Red Indian Line (RIL), a major late Ordovician suture between the Exploits and Notre Dame subzones, within the Notre Dame subzone, include the Cambrian (~ 510 Ma; e.g., Little Bay, Little Deer) and Cambro-Ordovician (~ 485 Ma; e.g., York Harbour, Betts Cove) ophiolite-hosted Cu-rich deposits, the ~ 485 Ma Au-enriched bimodal mafic deposits of the Rambler-Ming mining camp, and the ~ 471–465 Ma deposits of the Buchans-Roberts Arm belt (Fig. 1) (Dunning and Krogh 1985; Dunning et al. 1987; Jenner et al. 1991; Kean et al. 1995; van Staal 2007; Skulski et al. 2008, 2010). South of the Red Indian Line, within the Exploits subzone, VMS deposits occur in the ~ 513–509 Ma Tally Pond (TP) belt, ~ 511–506 Ma Long Lake belt, ~ 498–497 Tulks volcanic belt, and ~ 488–485 Ma Wild Bight (WB) Group (Figs. 1 and 2) (Dunning et al. 1991; MacLachlan and Dunning 1998a; MacLachlan and Dunning 1998b; Zagorevski et al. 2007b; Hinchey and McNicoll 2009; McNicoll et al. 2010; Zagorevski et al. 2010; Hinchey 2014).

The Duck Pond deposit is hosted within the Victoria Lake supergroup (Evans and Kean 2002). Historically, the Victoria Lake supergroup was divided into two

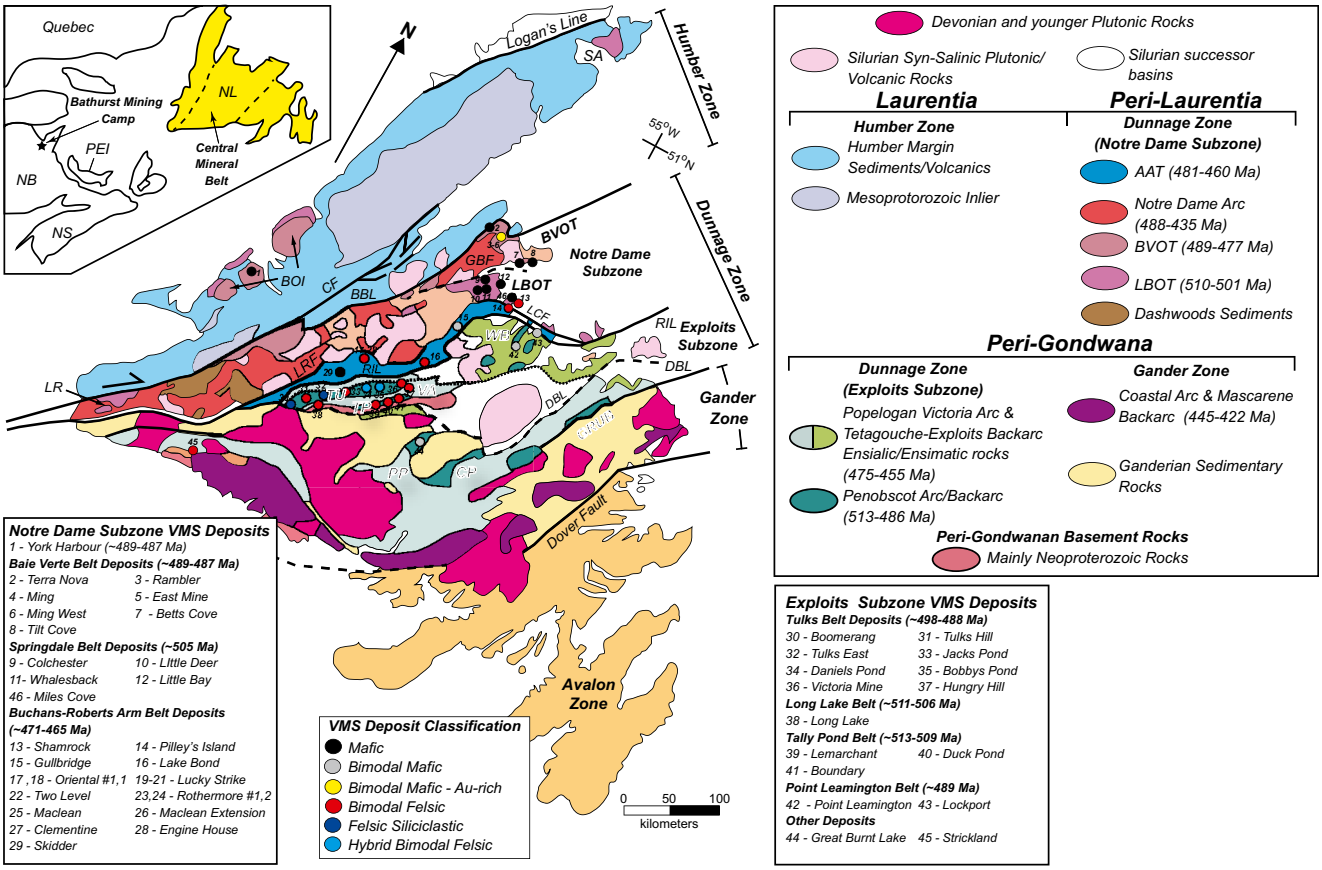

Fig. 1 Geological setting of the Newfoundland Appalachians with tectonostratigraphic zones and VMS deposits. Map modified from van Staal (2007) and van Staal and Barr (2012), with VMS classifications from Piercey (2007c) and Hinchey (2011). Abbreviations: BBL Baie Verte-Brompton Line, BOI Bay of Islands, BVOT Baie Verte oceanic tract, CF Cabot fault, CP Coy Pond Complex, DBL Dog Bay Line, GBF Green Bay fault, GRUB Gander River ultramafic belt, LBOT Lushs Bight oceanic tract, LCF Lobster Cove fault, LR Long Range, LRF Lloyds River fault, PP Pipestone Pond Complex, RIL Red Indian Line, SA St. Anthony, TP Tally Pond belt, TU Tulks volcanic belt, VA Victoria arc, WB Wild Bight Group

volcanic belts: the Tally Pond and Tulks volcanic belts (Evans and Kean 2002). More recently, it has been subdivided into six fault-bounded packages, including (Fig. 2): the Tally Pond group (~ 513–509 Ma) (Dunning et al. 1991; McNicoll et al. 2010), the Long Lake group (~ 511–506 Ma) (Zagorevski et al. 2007b; Hinchey 2014), Tulks group (~ 498–487 Ma) (Evans et al. 1990; Evans and Kean 2002), Sutherlands Pond group (~ 462 Ma) (Dunning et al. 1987), and Pats Pond and Wigwam Brook groups (~ 488 and ~ 455 Ma, respectively) (Zagorevski et al. 2007b). Volcanogenic massive sulfide deposits occur in the Tulks, Sutherlands Pond, Long Lake, and Tally Pond groups (Fig. 2) (Hinchey 2007, 2008; Hinchey and McNicoll 2009).

The Tally Pond group is host to the past-producing Duck Pond and Boundary VMS deposits, as well as the Lemarchant deposit (Fig. 2) (Squires et al. 1991, 2001; Evans and Kean 2002; Squires and Moore 2004; Piercey et al. 2014; Cloutier et al. 2017; Gill et al. 2016). The Tally Pond group has been subdivided into two informal formations: the Bindons Pond and Lake Ambrose formations (Rogers and van Staal 2002; Rogers et al. 2006). The Lake Ambrose formation is broadly equivalent to the Lake Ambrose basalts of Dunning et al. (1991) and is basalt-dominated with pillowed and massive flows, volcaniclastic rocks, and lesser volcanic and sedimentary rocks (Figs. 1 and 2) (Kean and Evans 1986; Evans and Kean 2002; Rogers and van Staal 2002; Rogers et al. 2006). The Bindons Pond formation is felsic-dominated with rhyolitic flows and volcaniclastic rocks, and carbonaceous clastic sedimentary rocks (Kean and Evans 1986; Evans and Kean 2002; Rogers and van Staal 2002; Rogers et al. 2006). There are notable problems with this bipartite stratigraphic subdivision, as evidenced by the intercalation of mafic and felsic volcanic rocks at the Lemarchant and Duck Pond deposits that have a range of ages from 513 to 509 Ma and occur at multiple stratigraphic levels (Squires et al. 1991, 2001; Evans and Kean 2002; Squires and Moore 2004; Piercey et al. 2014; Cloutier et al. 2017; Gill et al. 2016). Nevertheless, for simplicity and

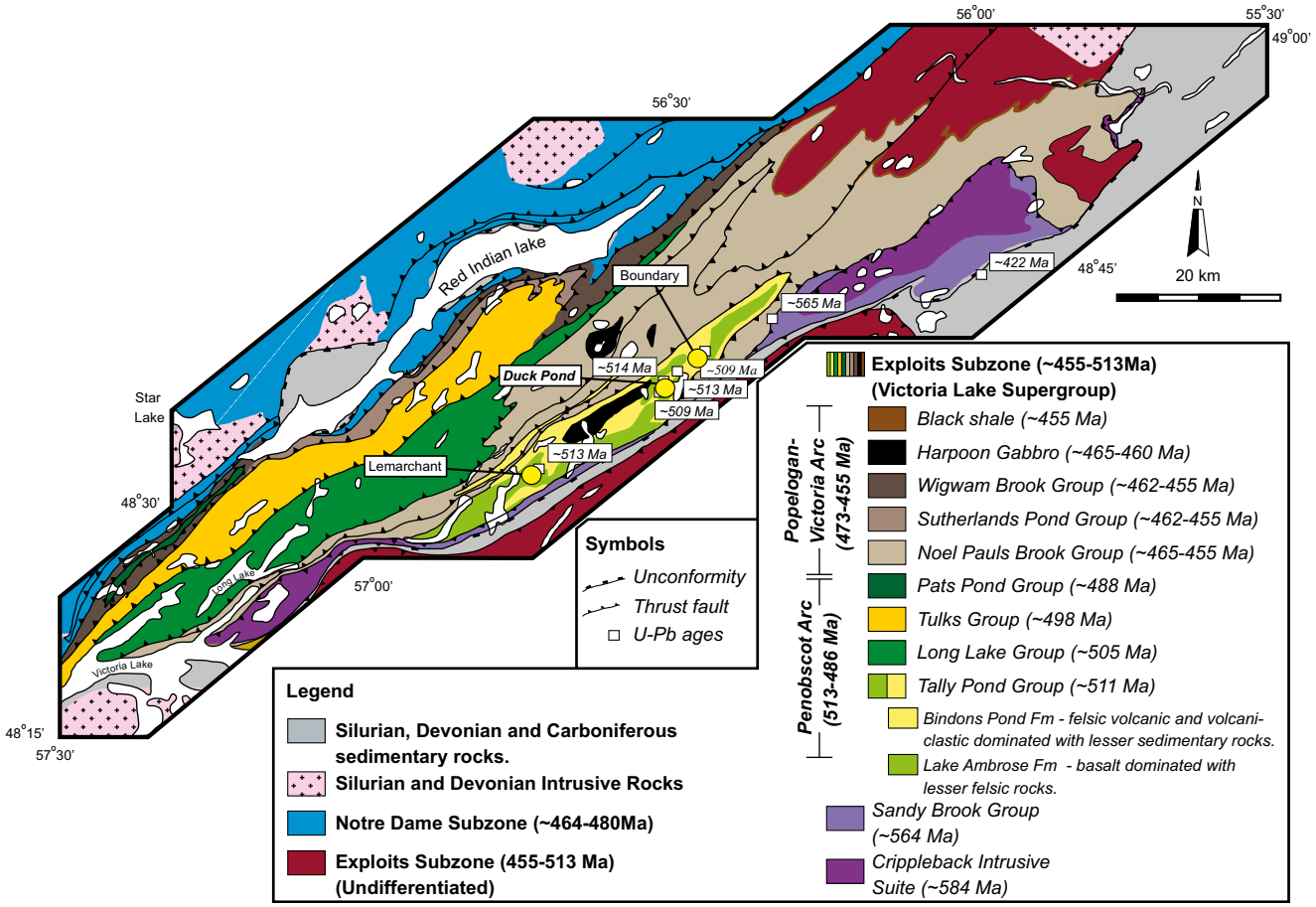

Fig. 2 Geological setting of the Victoria Lake supergroup and the Tally Pond group, with locations of VMS deposits in the Tally Pond group. Figure modified from McNicoll et al. (2010) and Cloutier et al. (2017)

correlation with regional stratigraphy, this division will be maintained here (Fig. 2) (Kean and Evans 1986; Evans and Kean 2002; Rogers and van Staal 2002; Rogers et al. 2006). In general, U-Pb zircon ages for the Lake Ambrose formation have yielded ~514–513 Ma ages, whereas the Bindons Pond formation has yielded ~509 Ma ages; the latter formation hosts mineralization at both the Duck Pond and Boundary deposits (Fig. 2) (McNicoll et al. 2010). The age of the host rocks at the Lemarchant deposit is presently uncertain but current age constraints (footwall felsic rocks have a U-Pb age of ~513 Ma) and stratigraphic relationships suggest that they are likely ~513 Ma and part of an older bimodal sequence within the Tally Pond group (~Lake Ambrose formation) (Dunning et al. 1991; Lode et al. 2016b; Cloutier et al. 2017).

Geological setting of the Duck Pond deposit

The Duck Pond deposit has been the focus of numerous studies (Kean 1985; Evans and Kean 1991, 2002; Squires et al. 1991, 2001; Moore 2003; Squires and Moore 2004). The deposit contains numerous lenses, but the bulk of the resource was mined from the Upper Duck lens, which consists of subseafloor replacement-style massive sulfides that comprise a Cu-Zn-rich core and a pyritic outer shell (Figs. 3 and 4). The mineralization occurs adjacent to the boundary between two fault-bounded panels: the mineralized block, which hosts the mineralization, and the upper block, which contains numerous sulfide-rich mudstones and minor mineralization (Figs. 3, 4, and 5). Rhyolitic rocks in the upper block have yielded U-Pb zircon ages ~514–512 Ma, whereas the mineralized block contains felsic rocks with ~509 Ma ages (McNicoll et al. 2010).

The two blocks contain fundamentally different volcanic and sedimentary facies. The mineralized block consists predominantly of massive, aphyric rhyolite that ranges from massive flows, to polygonally jointed rhyolite tuff breccias that host mineralization, to lapilli tuff and fine tuff (Figs. 3, 4, and 5) (Squires et al. 1991, 2001; Squires and Moore 2004; Piercey 2007a, b). The mineralized block also contains highly sheared carbonaceous argillite that contains variable amounts of volcanic

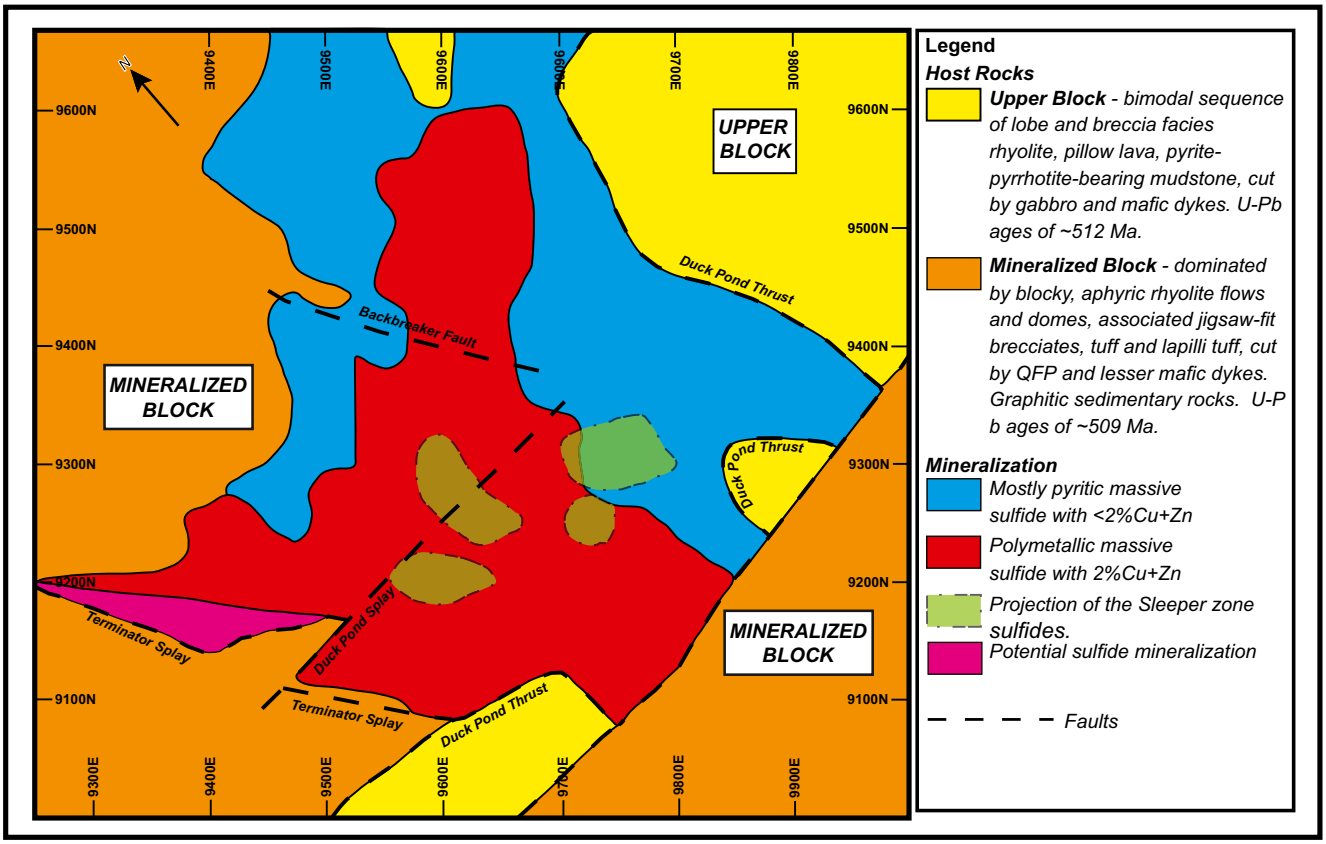

Fig. 3 Surface projection of the Duck Pond massive sulfide lenses and the associated geological host horizons. Diagram from Squires et al. (2001)

detritus and massive sulfide debris flows (Figs. 3, 4, and 5). The carbonaceous argillite stratigraphically overlies the mineralization but is the common locus of the Duck Pond thrust zone, a Silurian(?) thrust fault that separates the two blocks. Proximal to mineralization and 100s of meters into the footwall (and 100s of meters laterally), the rocks are hydrothermally altered with chlorite, with or without carbonate that occurs as dendritic and spotted dolomite within 10s of meters of mineralization, and sericite and quartz up to 200 m from mineralization (Figs. 4, 5, and 6). Footwall felsic tuffs from the Upper Duck lens in the mineralized block have yielded a U-Pb age of 508.7 ± 3.3 Ma (McNicoll et al. 2010).

The upper block contains a bimodal assemblage of rhyolite and basalt in roughly equal proportions, with lesser sedimentary horizons, and is cross-cut by mafic and felsic intrusive rocks. The rhyolitic rocks of the hanging wall are in conformable contact with basaltic rocks (Figs. 4 and 5) (Squires et al. 1991, 2001; Squires and Moore 2004; Piercey 2007a, b). The rhyolitic rocks are exceptionally preserved with well-developed flow banding that is locally flow-contorted and demarcated by spherulitic margins that grade into rhyolitic hyaloclastite and tuff (Piercey 2007a, b). Locally, there are well-developed lapilli tuff horizons with angular rhyolitic clasts, commonly found proximal to sulfide-rich mudstones and pillow lavas (Squires et al. 1991, 2001; Squires and Moore 2004; Piercey 2007a, b). The basaltic rocks are pillow lavas to massive flows that contain concentric rinds, local cooling cracks, minor chert, and angular basaltic hyaloclastite near their margins. The mafic rocks are interlayered with sulfide-rich mudstones (Figs. 4 and 5). Both the rhyolitic and basaltic rocks are altered, but to a lesser extent than the footwall rocks. The rhyolitic rocks have weak to moderate quartz alteration, and minor sericite and chlorite alteration of glassy margins. Locally, the flow-banded margins of the rhyolitic rocks have spherulites that are partially replaced by Fe-carbonate and Fe-oxides. The basaltic rocks are commonly altered with minor epidote, quartz, albite, and carbonate, with the latter filling amygdules, and the epidote-quartz-albite assemblage occurring as patches along pillow margins. For the most part, alteration in the upper block is patchy and not pervasive, except in proximity to sulfide-rich mudstones. The increased intensity of alteration of epidote-chlorite-quartz in basalts and quartz-sericite in felsic volcanic/volcaniclastic rocks proximal to the sulfide-rich mudstones is interpreted to be related to hydrothermal alteration associated with the hydrothermal system related to the emplacement of the mudstones.

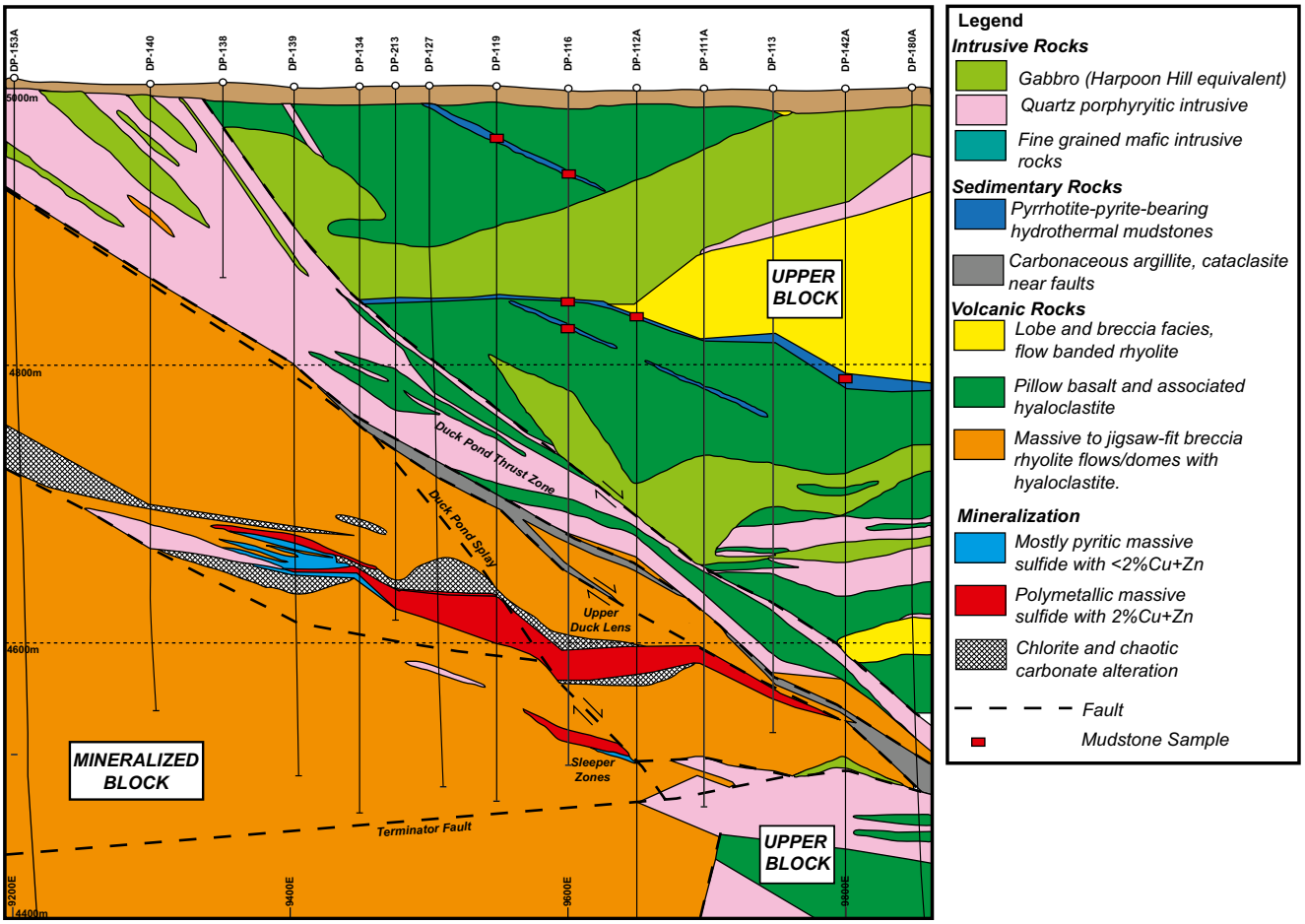

Fig. 4 Cross section 9200 N through the Duck Pond VMS deposit. Diagram modified from Squires et al. (2001). View into the section is toward the north

Notably, the mafic rocks in the upper block are strongly carbonate-altered within 50–70 m of the Duck Pond thrust zone (Fig. 4).

Intrusive rocks cut both the upper block and mineralized block. Massive quartz- and quartz-feldspar porphyritic intrusive rocks cross-cut the upper block and contain millimeter-scale to locally coarser feldspar and quartz phenocrysts, sharp margins with surrounding host rocks, and minor to moderate quartz and sericite alteration (Figs. 4 and 5). A cross-cutting quartz-porphyry intrusion in the upper block has yielded a 512 ± 2 Ma zircon age, an age that is younger, but overlaps, within error, of U-Pb ages for lobe and breccia facies rhyolites, in the upper block, which have ages that are ~ 514 ± 2 Ma (McNicoll et al. 2010). The upper block and the mineralized block proximal to the Duck Pond thrust zone are cut by gabbroic intrusive rocks and mafic dykes with non-arc chemistry (Squires and Moore 2004). The gabbroic intrusive rocks are coarse- to medium-grained, locally ophitic with preserved plagioclase and pyroxene, and are pristine, except in proximity to the Duck Pond thrust zone where they are Fe-carbonate-altered (Figs. 4 and 5). Finer-grained mafic dykes, which are interpreted to be coeval with the gabbros, intrude both the upper block, the mineralized block, mineralization, and the Duck Pond thrust zone (Figs. 4 and 5). In the areas away from the Duck Pond thrust zone, the mafic dykes are fine-grained and have sharp margins that are locally chilled. In proximity to mineralization and the Duck Pond thrust zone, they are strongly Fe-carbonate-altered and commonly contain sulfides, particularly along their margins. These dykes are also offset by the Duck Pond thrust zone (Figs. 4 and 5). The dykes and gabbroic rocks have been correlated with the Harpoon Hill gabbro, for which there is a 465 ± 1-Ma age (Pollock 2004); this suggests that movement on the thrust zone is post-465 Ma.

Sulfide-rich mudstones

Sulfide-rich mudstones (i.e., > 25% sulfide) in the Duck Pond VMS deposit are hosted exclusively within the upper block. The upper block rocks pre-date the main mineralization event at Duck Pond by ~ 4 m.y., but based on

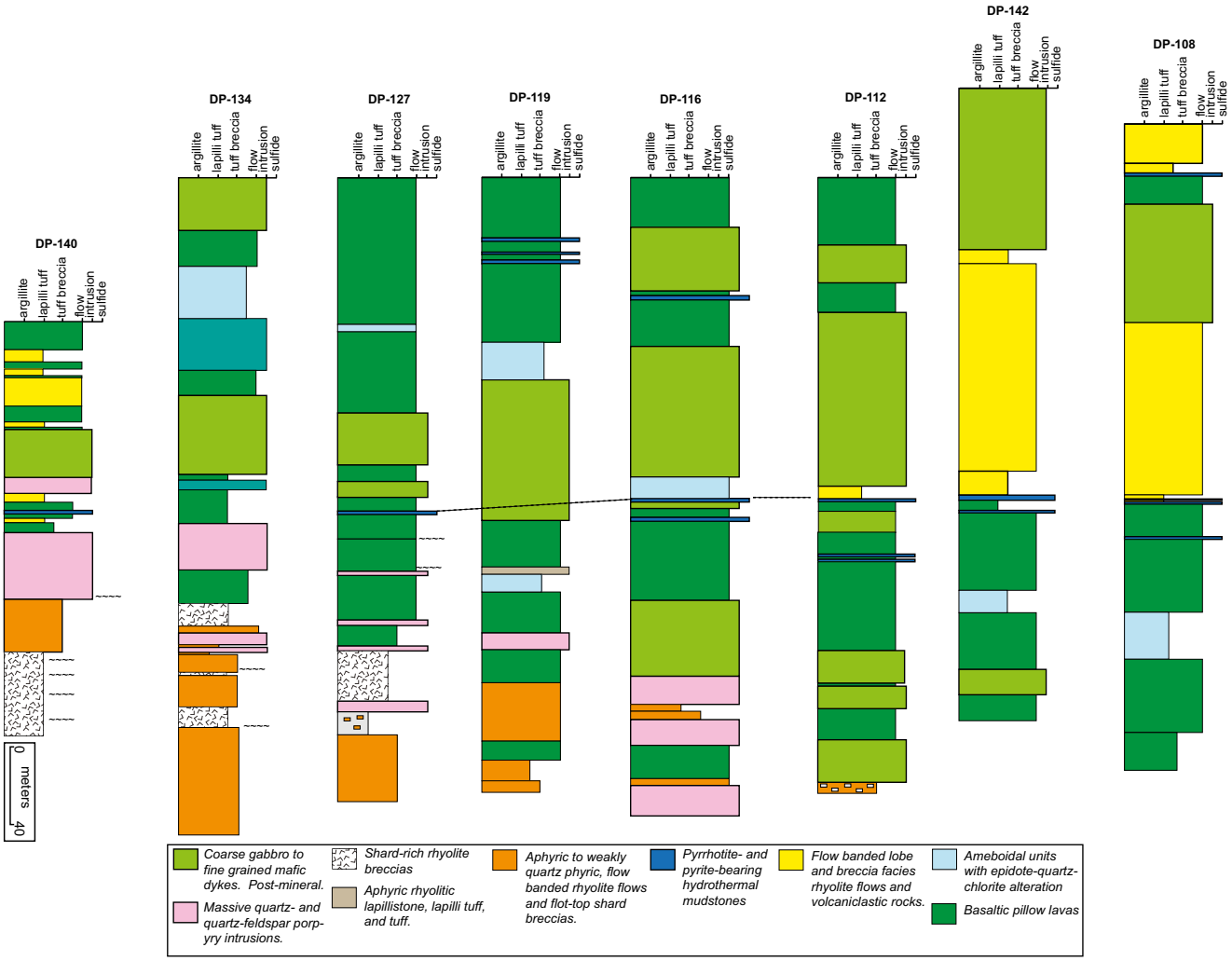

Fig. 5 Partial lithostratigraphic columns along section 9200 N. Drill hole numbers correspond to those that are outlined on Fig. 4. Notably, hydrothermal sedimentary rocks occur at numerous stratigraphic levels and in different host assemblages. They predominantly occur in basaltic rocks and also along contacts between basaltic horizons and rhyolitic horizons

stratigraphic arguments and similarities with host stratigraphy, they are likely coeval with hydrothermal mudstones in the Lemarchant deposit (Lode et al. 2015, 2016a, b; Cloutier et al. 2017). The hydrothermal mudstones are pyrrhotite-rich and found at numerous stratigraphic levels (Figs. 4, 5, and 6) and have minor variability in texture and composition (Fig. 6). They are variably laminated and are comprised of a number of facies, including: (1) finely laminated pyrrhotite that is brassy in color and intergrown with black mudstone (Fig. 6a, b); (2) laminated to massive pyrrhotite with minor pyrite and chalcopyrite, often with rounded mudstone balls (Fig. 6c); (3) finely interlaminated pyrrhotite and black mud, with or without felsic ash layers (Fig. 6d); (4) hydrothermal mudstones with contorted hydrothermal layers (Fig. 6e); (5) carbonaceous mud-rich layers with clots of pyrrhotite and intergrown with volcanic clasts; and (6) ochre-like horizons rich in pyrrhotite, but with a minor millimeter-scale surface rind of rusty weathering (Fig. 6f, g).

The hydrothermal mudstones occur in two main stratigraphic positions: (1) solely within pillow lavas as interflow horizons and (2) at contacts between basaltic pillow lavas and rhyolitic lavas (Figs. 4, 5, and 6). In cases where pillow lavas are the hosts, the mudstones occur along pillow margins, and within a single drill hole, they can occur at multiple horizons between successive pillowed flows (Fig. 5). The pillow lavas proximal to the sulfide-rich mudstones have variably pervasive epidote, quartz, and chlorite alteration with minor pyrite. In addition, there are very distinctive ameboidal horizons that have irregularly shaped textures with globular chlorite intergrown with quartz and epidote (Figs. 5 and 6h); these horizons do not occur anywhere else in the upper block or the

◀ **Fig. 6** **a**, **b** Fine-grained pyrrhotite-bearing hydrothermal sedimentary rock with fine pyrrhotite within a carbonaceous matrix. **c** Pyrrhotite- and chalcopyrite-bearing hydrothermal sedimentary rock with globular carbonaceous mudstone along pillow margins. **d** Finely laminated mudstone with interlaminated pyrrhotite and black argillite. **e** Contorted, rusty pyrrhotite-bearing hydrothermal sedimentary rock on the edge of a pillow lava. **f** Black muddy horizons with pyrrhotite blebs (transported?) with minor rhyolitic volcanic clasts within a matrix of carbonaceous mudstone. **g** Rusty, ochre-like hydrothermal mudstone along a pillow lava margin. **h** Rusty hydrothermal mudstone along a pillow lava margin. Overlying, this unit as presented in the upper part of the photograph is an angular rhyolitic volcaniclastic unit that is commonly found proximal to hydrothermal mudstones when near rhyolite flows. **i** Ameboidal, spotted epidote-quartz-chlorite-altered mafic horizons in pillow lavas. These textures and mineral assemblages are often found in mafic units proximal to the hydrothermal mudstones. **j** Close-up of the angular to subangular, matrix- to clast-supported rhyolitic volcaniclastic horizon found proximal to some hydrothermal mudstones with quartz and sericite alteration

mineralized block except near mudstone and are interpreted to be hydrothermal alteration assemblages associated with mudstone deposition. In the case where the hydrothermal mudstones occur proximal to the contacts between felsic and mafic rocks, the basalts have similar alteration and ameboid textures (Fig. 5). When near rhyolite-basalt contacts, there are felsic breccias containing angular to subangular fragments of rhyolite that are locally flow-banded, within a matrix of chlorite-sericite-altered felsic ash (Figs. 5 and 6h, j). These felsic horizons are commonly strongly sericite- and quartz-altered with minor chlorite alteration of the finer-grained ash proximal to the hydrothermal mudstones.

The hydrothermal mudstones consist of varying abundances of pyrrhotite with lesser pyrite, chalcopyrite,

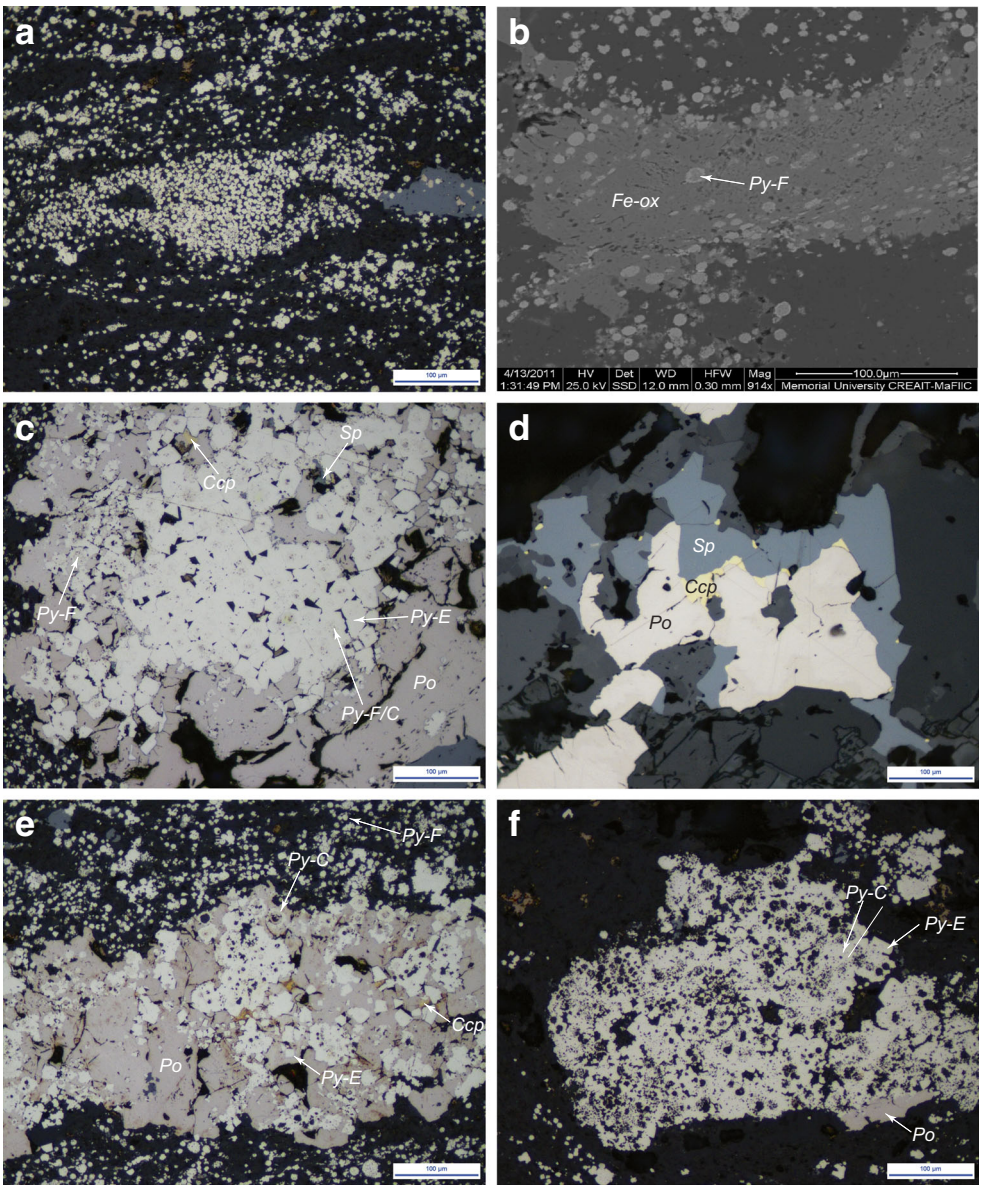

Fig. 7 Photomicrographs of textures and mineral assemblages in the Duck Pond hydrothermal mudstones. **a** Framboidal pyrite within a siliceous to carbonaceous matrix with minor sphalerite (gray). **b** Fe-oxide particle (hematite) overgrown by framboidal pyrite. It is interpreted that framboidal pyrite is diagenetic and formed from original Fe-oxide/oxyhydroxide particles. **c** Euhedral pyrite grains with relict framboidal pyrite cores and surrounded by diagenetic pyrrhotite, with minor chalcopyrite. **d** Blebby pyrrhotite, chalcopyrite, and sphalerite. These are interpreted to be diagenetic based on textural relationships and sulfur isotope systematics (Piercey et al. 2013). **e** Framboidal pyrite in a siliceous/carbonaceous matrix with diagenetic pyrrhotite and some subhedral pyrite. There are relict colloform pyrite textures that are partly overgrown by euhedral pyrite and there are euhedral pyrite grains that are interpreted to be of hydrothermal origin. **f** Relict colloform pyrite partly overgrown by euhedral pyrite and minor diagenetic pyrrhotite. The colloform pyrite is interpreted to be of hydrothermal origin. All images are under reflected light except **b**, which is a back scatter electron image. Py-F framboidal pyrite, Py-E euhedral pyrite, Py-C colloform pyrite, Po pyrrhotite, Ccp chalcopyrite, Sp sphalerite

sphalerite, and arsenopyrite. They are hosted within a matrix dominated by quartz, chlorite, organic material, and much lesser Fe-oxides/hematite, calcite, dolomite, Fe-carbonate, K-feldspar, celsian, apatite, monazite, and zircon. There are also distinctive textural variations in the sulfide/oxide species (Fig. 7). The samples contain abundant framboidal pyrite that forms both clusters and solitary grains throughout the matrix of the mudstones (Fig. 7a). These framboids locally overgrow hematite (Fe-oxides) (Fig. 7b) suggesting that they are diagenetic and likely replaced pre-existing hydrothermal Fe-oxides/oxyhydroxides. Moreover, the framboids are overgrown by new pyrite grains that are anhedral to euhedral, and/or are converted to sheets of anhedral pyrrhotite (Fig. 7c, d). Pyrrhotite sheets and the framboids are also found with anhedral sphalerite and chalcopyrite grains (Fig. 7a, d). All of these phases have S-isotopic signatures that suggest that their sulfur budgets were predominantly biogenically derived (Piercey et al. 2013). In contrast, some sulfides have textures indicative of potential hydrothermal origins. Well-developed euhedral pyrite that is found proximal to the pyrrhotite sheets is texturally distinctive (Fig. 7e, f) and has S-isotopic signatures indicative of S derived from thermochemical sulfate reduction of seawater sulfate (Piercey et al. 2013). Moreover, colloform pyrite and micro-chimneys found in the hydrothermal mudstones are similar to those found in exhalative seafloor massive sulfides (Eldridge et al. 1983).

Lithogeochemistry

Samples for lithogeochemistry were taken from various drill holes within the deposits. Samples were collected from full or half-cut drill core and roughly 10–15 cm in length; all core samples were NQ-size (47.6 mm diameter) cores. Samples were prepared and analyzed at the Ontario Geoscience Laboratories (OGL) in Sudbury, Canada. Samples were crushed and pulverized using a standard jaw crusher and an agate pulverizer. Major elements were measured by X-ray fluorescence on pressed powder pellets and LOI was determined by weight loss. Trace elements, including the high field strength elements (HFSE), rare earth elements (REE), low field strength elements (LFSE), and base and volatile metals, were determined using both inductively coupled plasma emission spectroscopy (ICP-ES) and mass spectrometry (ICP-MS) following a closed beaker, multi-acid digestion to ensure all resistant phases were dissolved, utilizing the methods of Burnham and Schweyer (2004). Mercury analyses were determined via cold vapor atomic absorption spectroscopy (CV-AAS). Total CO_2 and S were analyzed via infrared spectroscopy, $C_{inorganic}$ was determined by Chittick methods, and $C_{organic}$ was determined via the difference in C_{total} (derived from total CO_2 and $C_{inorganic}$). Precision and accuracy of analytical data at the OGL has been previously reported in Ruks et al. (2006), MacDonald et al. (2005), and DeWolfe et al. (2009). Lithogeochemical data are presented in Electronic Supplementary Materials (ESM Table 1) and Figs. 8, 9, 10, 11, 12, 13, 15, 16, and 17. Due to the sulfide-rich nature of these samples, major element data have been plotted on a volatile-free basis on major element diagrams (e.g., Figs. 8 and 10).

Results

Major elements

The major element systematics of the Duck Pond upper block mudstones are shown in Fig. 8. On the A-CN-K plot (Nesbitt and Young 1984; Nesbitt 2003), the majority of samples lie on an array between illite-muscovite and hornblende-plagioclase (Fig. 8a). In A-CNK-FM space, the samples lie primarily between the smectite and the oxide-sulfide-node; two samples are proximal to the carbonate node (Fig. 8b). The chemical index of weathering in the Duck Pond mudstones [$CIW = 100 \times Al_2O_3/(Al_2O_3 + Na_2O + K_2O + CaO)$] (Nesbitt and Young 1984; Nesbitt 2003) range from ~ 40 to 70 and have an inverse relationship with CaO (Fig. 8d). The higher CIW values are associated with higher Zr, potentially indicating a greater felsic detrital component in high CIW samples (Fig. 8d).

Sediment provenance: detrital components

To evaluate potential detrital components in the Duck Pond upper block mudstones, select HFSE, REE, and compatible elements (e.g., Sc) are utilized (Bhatia and Crook 1986; McLennan et al. 1993; McLennan et al. 2003) because these elements are relatively immobile during hydrothermal alteration and metamorphism and retain original provenance signatures (MacLean 1990). In terms of Th-La-Sc-Zr compositions, the Duck Pond upper block mudstones lie within the fields for both continental and oceanic arcs (Fig. 9a, b), consistent with the regional geological setting for the Tally Pond group (Rogers et al. 2006). They also lie on an array that extends from the upper crust to the depleted mantle, and along a mixing line between mafic and felsic rocks (Fig. 9c). The samples also have upper crust normalized La/Sm ratios that are near 1, but slightly below the upper crust control line (Fig. 9d).

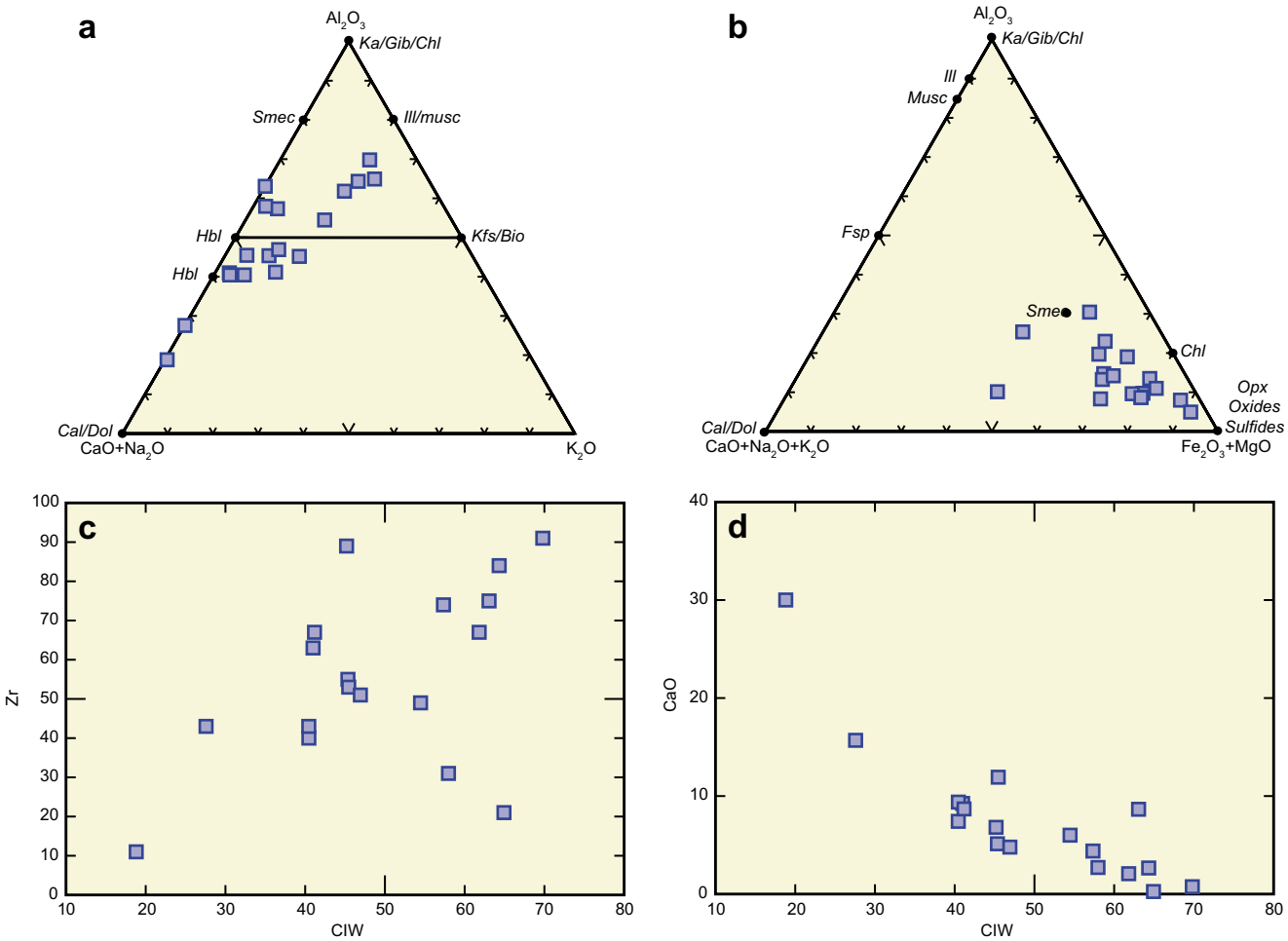

Fig. 8 **a** ($CaO+Na_2O$)–Al_2O_3–K_2O and **b** ($CaO+Na_2O+K_2O$)–Al_2O_3–(Fe_2O_3+MgO) plots of Nesbitt (2003) and Nesbitt and Young (1984). Chemical index of weathering versus **c** CaO and **d** Zr. All data are recalculated as volatile free

Hydrothermal and adsorbed (seawater) components

The hydrothermal nature of the Duck Pond upper block mudstones is illustrated in Fig. 10. All samples have high Fe/Ti ratios at a given Al/Al+Fe+Mn content (Fig. 10a) and lie within the hydrothermal field on the Fe-Al-Mn plot (Fig. 10b). The mudstones have Fe_2O_3 ranging from ~ 10 to 55%, S from ~ 5 to 20%, and Pb (~ 20–100 ppm), Zn (~ 300–3000 ppm), Cu (~ 100–1000 ppm), Co (~ 10–100 ppm), Ba (10–200 ppm), and Hg (100–3000 ppb) (ESM Table 1). They also have elevated Ba/Al_2O_3 and $Zn+Hg/Al_2O_3$ ratios similar to distal hydrothermal sedimentary rocks found elsewhere in the Tally Pond belt (Fig. 10c; e.g., Lode et al. 2015, 2016b).

The Post-Archean Australian Shale (PAAS)-normalized plot shows that the hydrothermal mudstones have a pattern similar to oxygenated seawater with depleted light REE (LREE), negative Ce anomalies (Ce/Ce* = 0.40–0.86; average = 0.58), flat to weakly positive Eu anomalies (Eu/Eu* 1.02–1.86; average = 1.22), a positive Y anomaly, and high Y/Ho ratios (Fig. 11) (Bau 1996, 1999; Bau et al. 1996; Nozaki et al. 1997). There is also an inverse correlation between the high Y/Ho values and the degree of Ce/Ce* depletion (Fig. 11). Given that REE and Y can be strongly affected by detrital minerals, including zircon (high Ce/Ce*) and clays (high Al_2O_3 and Fe_2O_3), Y/Ho and Ce/Ce* are plotted against Al_2O_3, an indicator of clay minerals (sericite, chlorite), and Zr, an indicator of heavy minerals (zircon), both elements reflective of potential detrital sediment component (see Kamber and Webb 2001; Kamber et al. 2004). The Y/Ho and Ce/Ce* compositions of the mudstones show little overlap with those of basalt and rhyolite and no correlative relationship with elements indicative of detrital sedimentary material; therefore, it suggests that the Y/Ho and Ce/Ce* signatures are primary signatures of the hydrothermal sediments that are largely unaffected by detrital sediment contamination (ESM Fig. 1).

The Y/Ho and Ce/Ce* values of the Duck Pond upper block mudstones are plotted against oxyanions in ESM

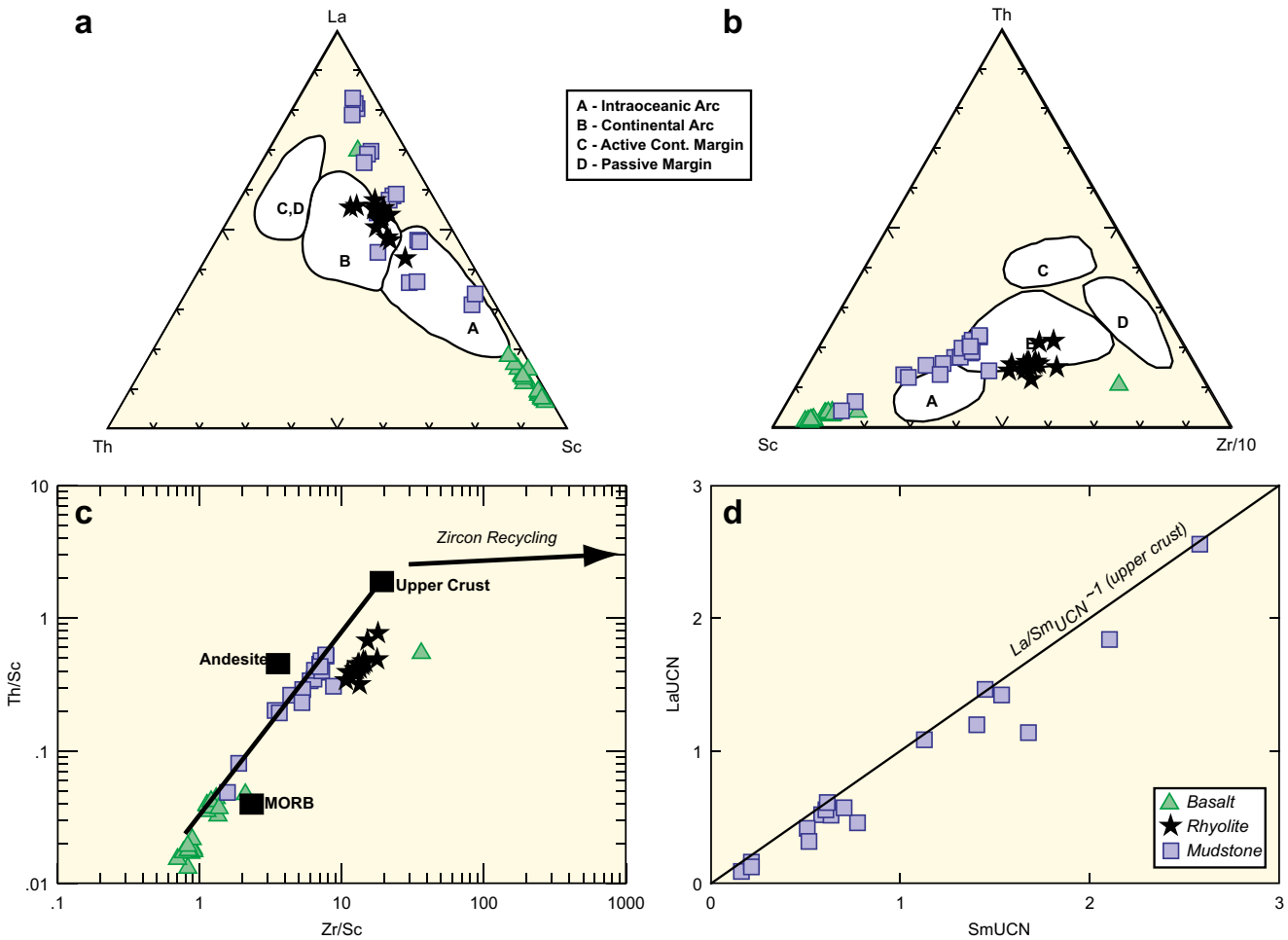

Fig. 9 Discrimination diagrams for sedimentary rocks. **a** Th-La-Sc diagram and **b** Th-Zr-Sc diagram of Bhatia and Crook (1986). **c** Th/Sc-La/Sc diagram of McLennan et al. (1993, 2003). **d** Upper crust normalized La-Sm plot. Values for the upper crust from McLennan (2001). Shown for comparison are basaltic and rhyolitic rocks from the upper block (Piercey, unpublished data)

Fig. 2. The Y/Ho and Ce/Ce* ratios correlate with these oxyanions, which are elements that are commonly associated with adsorption and element scavenging onto vent particles in modern hydrothermal systems (Feely et al. 1991, 1998; German and Von Damm 2003). In particular, Y/Ho shows positive correlations and Ce/Ce* shows negative correlations with P_2O_5, U, and Cd (ESM Fig. 2).

Redox-sensitive elements

Elements sensitive to the redox state of the oceanic bottom waters during deposition of the Duck Pond upper block mudstones are presented in Fig. 12. Notably, most samples have Mn values with a large range, but with an average value of ~ 1500 ppm, typical of sedimentary rocks deposited from an oxygenated water column (Fig. 12a) (Calvert and Pedersen 1993; Quinby-Hunt and Wilde 1994; Calvert and Pedersen 1996). Paradoxically, the samples also have elevated V/(V+Ni) ratios, V/Cr, U/Th, and Ni/Co ratios, which suggest deposition under anoxic conditions (Fig. 12) (Jones and Manning 1994; Quinby-Hunt and Wilde 1994). Despite the latter, the negative Ce anomalies shown in Fig. 11 (Ce/Ce* < 1) are similar to sediments/shales deposited under oxic conditions (de Baar et al. 1988; German et al. 1991b; Goodfellow et al. 2003b).

Discussion

Geochemical dynamics of Duck Pond hydrothermal sedimentary rock formation

The lithogeochemical signatures from the Duck Pond sulfide-rich mudstones provide insight into the nature of

Fig. 10 **a** Fe/Ti versus Al/Al+Fe+Mn. **b** Fe-Al-Mn plot for evaluating the relative contributions of hydrothermal versus detrital material within hydrothermal sedimentary rocks (Boström and Peterson 1969; Boström et al. 1972; Boström 1973). **c** Ba/Al_2O_3–$(Zn+Hg)/Al_2O_3$. Proximal and distal fields in **c** are based on data from the regionally correlative mudstones in the Lemarchant deposit as defined by Lode et al. (2015) ▶

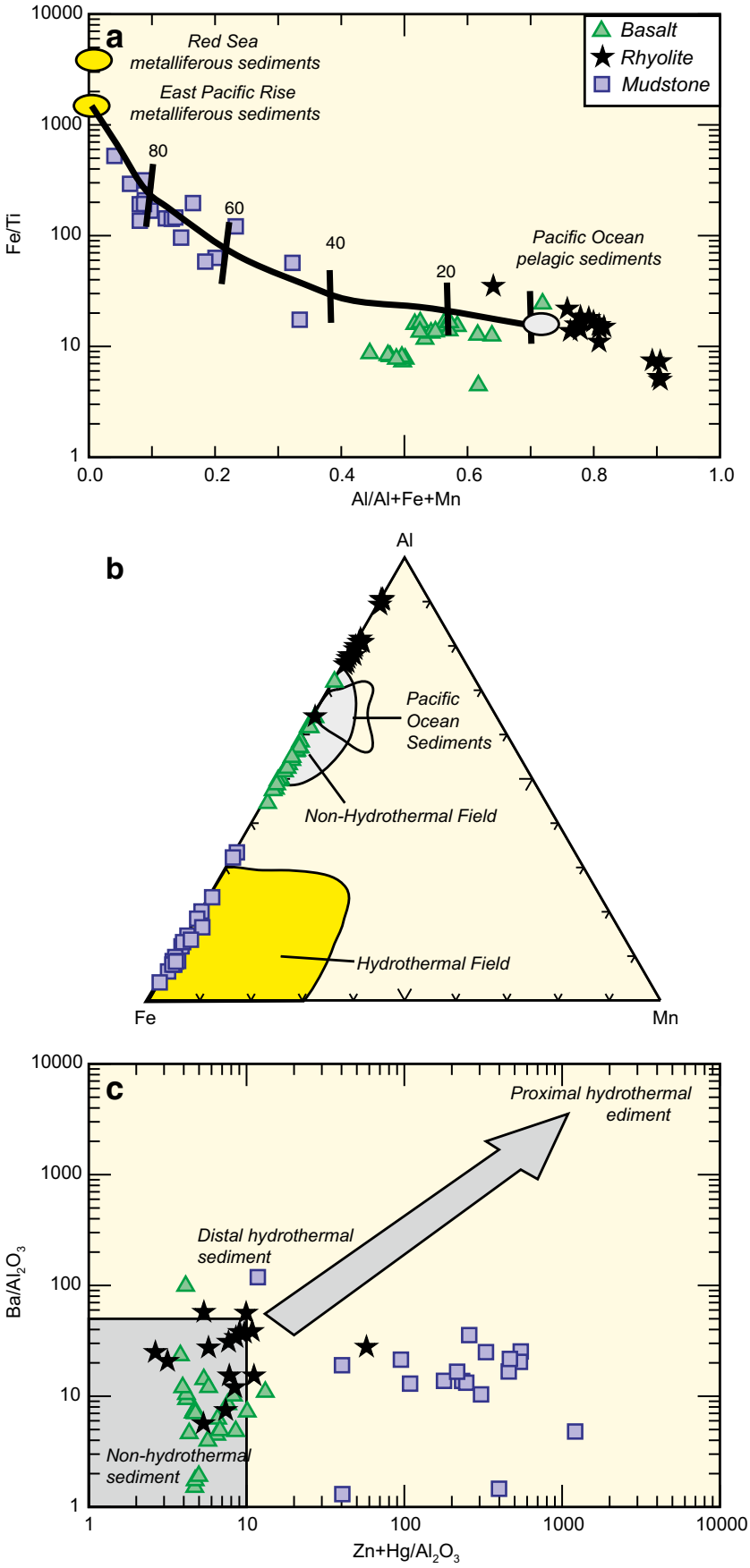

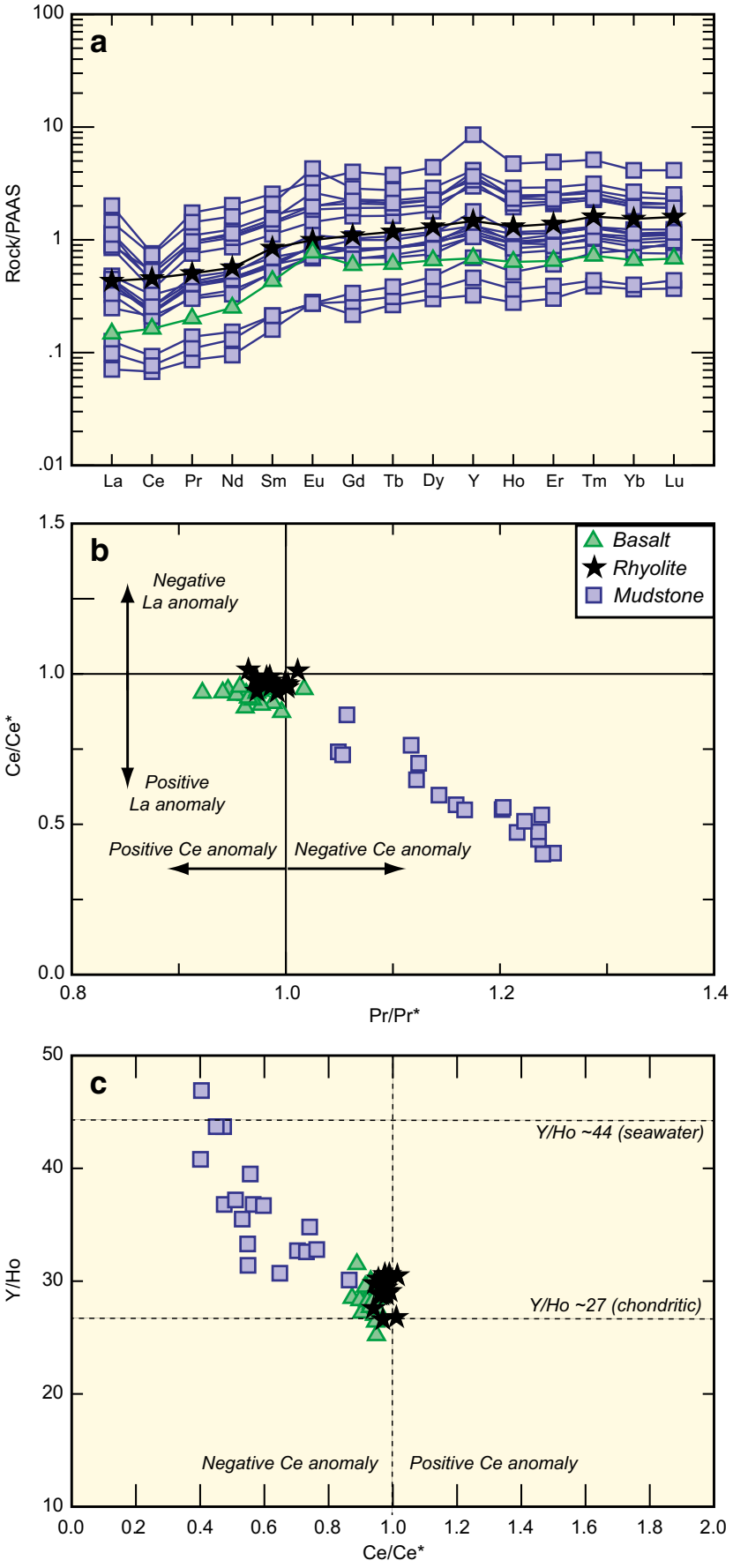

◀ **Fig. 11** **a** Post-Archean Australian Shale (PAAS)-normalized REE+Y plot of Duck Pond upper block mudstones. In **a**, note the negative Ce anomalies and positive Y/Ho anomalies. **b** The Ce anomalies in **a** are also accompanied by positive La anomalies, features that are very similar to modern seawater, and there is an inverse correlation with lower Ce/Ce* and higher Y/Ho ratios (**c**). The negative Ce anomalies and high Y/Ho values for the Duck Pond hydrothermal sedimentary rocks are signatures similar to modern seawater suggesting that these sediments had sufficient residence time to scavenge REE and Y from ambient seawater. Diagram in **b** is from Kamber and Webb (2001). Y/Ho values for various reservoirs in **c** are from Bau (1996) and Nozaki et al. (1997). $Ce/Ce^* = Ce_{SN}/(0.5La_{SN} + 0.5Pr_{SN})$ and $Pr/Pr^* = Pr_{SN}/(0.5Ce_{SN} + 0.5Nd_{SN})$; SN = PAAS-normalized values (Kamber and Webb 2001)

hydrothermal activity and their physicochemical conditions of formation. The chemistry of hydrothermal sedimentary rocks reflects the complex contribution of elements from: (1) clastic sedimentary detritus; (2) hydrothermal fluid discharge; and (3) elements adsorbed from seawater onto hydrothermal particles (German et al. 1990, 1991a; Feely et al. 1991; Peter and Goodfellow 1996; Feely et al. 1998; German and Von Damm 2003; Peter 2003; Peter et al. 2003). The element proportioning and distribution amongst the latter is also controlled strongly by ocean redox conditions, as well as the temperature of hydrothermal discharge (Peter 2003). The detrital component within the Duck Pond mudstones comes from the surrounding basaltic and rhyolitic rocks, as samples with elevated Al_2O_3, low Fe/Al ratios, and incompatible element signatures lie along mixing lines between hydrothermal sediment and surrounding host rhyolite and basalt (Fig. 9). Having a detrital contribution from these sources is not surprising in light of their stratigraphic position in the upper block (Figs. 4 and 5).

Despite a detrital component, the Duck Pond upper block mudstones have hydrothermal Fe/Al ratios, Fe-Mn-Al systematics (Fig. 10), and elevated Zn, Pb, Cu, Hg, and Ba contents (ESM Table 1), similar to signatures found in modern and ancient hydrothermal sedimentary rocks (German et al. 1991a; Peter and Goodfellow 1996; Peter 2003; Peter et al. 2003; Edmonds and German 2004; Hrischeva and Scott 2007; Hrischeva et al. 2007; Slack et al. 2009). However, compared to modern high-temperature vent fluids, the Duck Pond upper block mudstones have low Eu/Eu* values (1.02–1.86; average = 1.22) and negative to flat Eu and negative Ce anomalies on PAAS- and chondrite-normalized REE plots, which differs from modern high-temperature vent fluids (Fig. 13) (Michard et al. 1983; Sverjensky 1984; Michard 1989; Mitra et al. 1994; Mills 1995; Douville et al. 1999). The REE-Y signatures of the mudstones are more similar to hydrothermal plume-derived Fe-oxide/oxyhydroxide precipitates (i.e., hydrothermally derived muds) and Fe-oxide/oxyhydroxide plume particles, but with less pronounced positive Eu anomalies (Figs. 11 and 13). Sverjensky (1984) illustrated that at elevated temperatures (i.e., > 250 °C) in aqueous fluids, Eu^{2+} should be the dominant species and high-temperature fluids should have $Eu/Eu^* \gg 1$. This is also recorded in high-temperature vent fluids (Michard et al. 1983), and modern and ancient hydrothermal sedimentary rocks (German et al. 1993; Peter 2003). Thus, the generally low Eu/Eu* values and the lack of pronounced positive Eu anomalies in the Duck Pond hydrothermal mudstones are consistent with deposition from low-temperature fluids with $T < 250$ °C (Sverjensky 1984; Peter 2003). Further, while it could be argued that part of their flat to weakly positive Eu/Eu* signature is due to detrital contamination, the higher total REE-Y values and higher Eu/Eu* than the surrounding basaltic and rhyolitic host rocks argue against Eu anomaly controlled by detritus and imply that the Eu/Eu* is of hydrothermal origin.

Negative Ce anomalies that characterize the Duck Pond upper block mudstones are also prevalent in some modern vent particles and particle-derived sediments and are similar to the signatures found in modern oxygenated seawater (Fig. 13) (Elderfield and Greaves 1982; Elderfield et al. 1988; de Baar et al. 1991; German et al. 1991a; Nozaki and Alibo 2003). In modern hydrothermal environments, buoyant Fe-oxide/oxyhydroxide particles in hydrothermal plumes adsorb and scavenge REE from seawater, resulting in particles and subsequent hydrothermal sediments with seawater-like REE-Y signatures (Figs. 13 and 14) (German et al. 1990, 1991a, 1993; Mitra et al. 1994; Bau 1996, 1999; German and Von Damm 2003; Edmonds and German 2004; Chavagnac et al. 2005). German et al. (1990) and Edmonds and German (2004) further illustrated that the longer the interaction between particles and ocean water, the more REE-enriched and more seawater-like their signatures became (i.e., low Ce/Ce* and low Eu/Eu*). It is therefore reasonable to assume that the Ce anomalies and seawater-like REE-Y signatures in the Duck Pond mudstones reflect the REE-Y signatures of oxygenated mid-Cambrian seawater that were inherited from Fe-oxide/oxyhydroxide scavenging (Figs. 13 and 14).

The scavenging of elements from seawater via particle adsorption is also consistent with the Y/Ho systematics of the mudstones. Yttrium and Ho are geochemical twins and generally behave coherently during most earth processes, exhibiting charge and radius-controlled (CHARAC) behavior, retaining near-chondritic ratios (Y/Ho ~27) (Bau 1996) (Fig. 11). Moreover, in hydrothermal vent fluids, the Y/Ho ratios are generally similar to chondritic values and Y and Ho are not fractionated from one another during the generation of seafloor hydrothermal fluids (Fig. 11) (Douville et al. 1999). In contrast, seawater has distinctly non-CHARAC behavior with super-chondritic Y/Ho values (> 44) (Fig. 11) (Bau

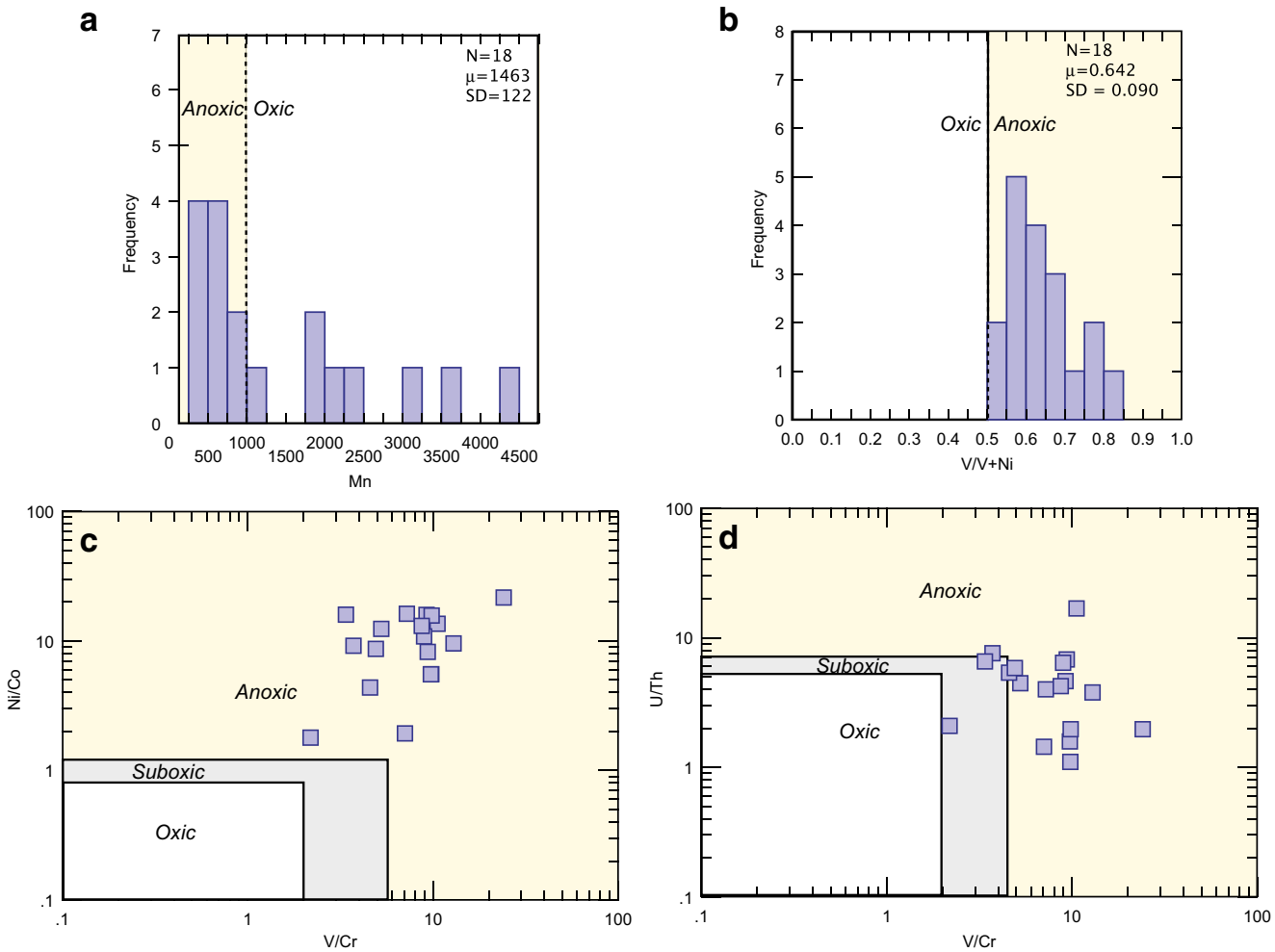

Fig. 12 Redox-sensitive trace element plots. Histograms of **a** Mn and **b** V/(V+Ni). **c** Ni/Co versus V/Cr. **d** U/Th versus V/Cr. Ratios defining oxic, suboxic, and anoxic fields in **b** and **c** are from Jones and Manning (1994)

1996; Nozaki et al. 1997). The Duck Pond mudstones have Y/Ho values that range from chondritic, with either hydrothermal input or detrital sediment leading to low Y/Ho, to those with the most super-chondritic ratios (Fig. 11), which are interpreted to reflect adsorption of the Y/Ho from seawater onto hydrothermal particles (Fig. 14) (Bau 1996, 1999; Nozaki et al. 1997).

Although the REE-Y systematics of the hydrothermal mudstones are consistent with scavenging from oxygenated seawater, many of the redox-sensitive transition elements have signatures that are indicative of deposition under anoxic conditions (Fig. 12). However, the degree of enrichment of these "anoxic" indicators coincides with lower Ce/Ce* and higher Y/Ho ratios, typical of oxygenated seawater (Elderfield and Greaves 1982; Elderfield et al. 1988; Nozaki et al. 1997; Alibo and Nozaki 1999) (Figs. 15 and ESM Fig. 2). Moreover, in anoxic basins, bottom waters and associated fine-grained sedimentary rocks typically have Y/Ho values that are slightly super-chondritic (i.e., Y/Ho ~ 44) to sub-chondritic (i.e., < 44) and Ce/Ce* values that are ≥ 1 (de Baar et al. 1988; German et al. 1991b; Bau et al. 1997), the opposite of what is observed in the Duck Pond hydrothermal mudstones. Thus, the enrichment in redox-sensitive trace elements indicative of anoxic conditions, yet REE-Y systematics indicative of an oxygenated water column, is problematic. The enrichment in elements like V, Ni, Cr, Co, U, and Cd could be related to their adsorption onto organic material within the sediment pile during diagenesis (Tribovillard et al. 2006). Notably, some of the samples presented herein have very high C_{org} contents (> 4% C_{org}); however, the relationship between elements indicative of anoxic conditions and C_{org} (Fig. 16) shows little correlation (V/(V+Ni), U/Th), weak positive correlation (Mn), or weak negative correlations (Ni/Co), features opposite to that expected by sediments deposited under anoxic conditions, and also suggests that organic matter adsorption in the sediment pile was not the main controller of Mn-V-Ni-U concentrations in the sulfide-

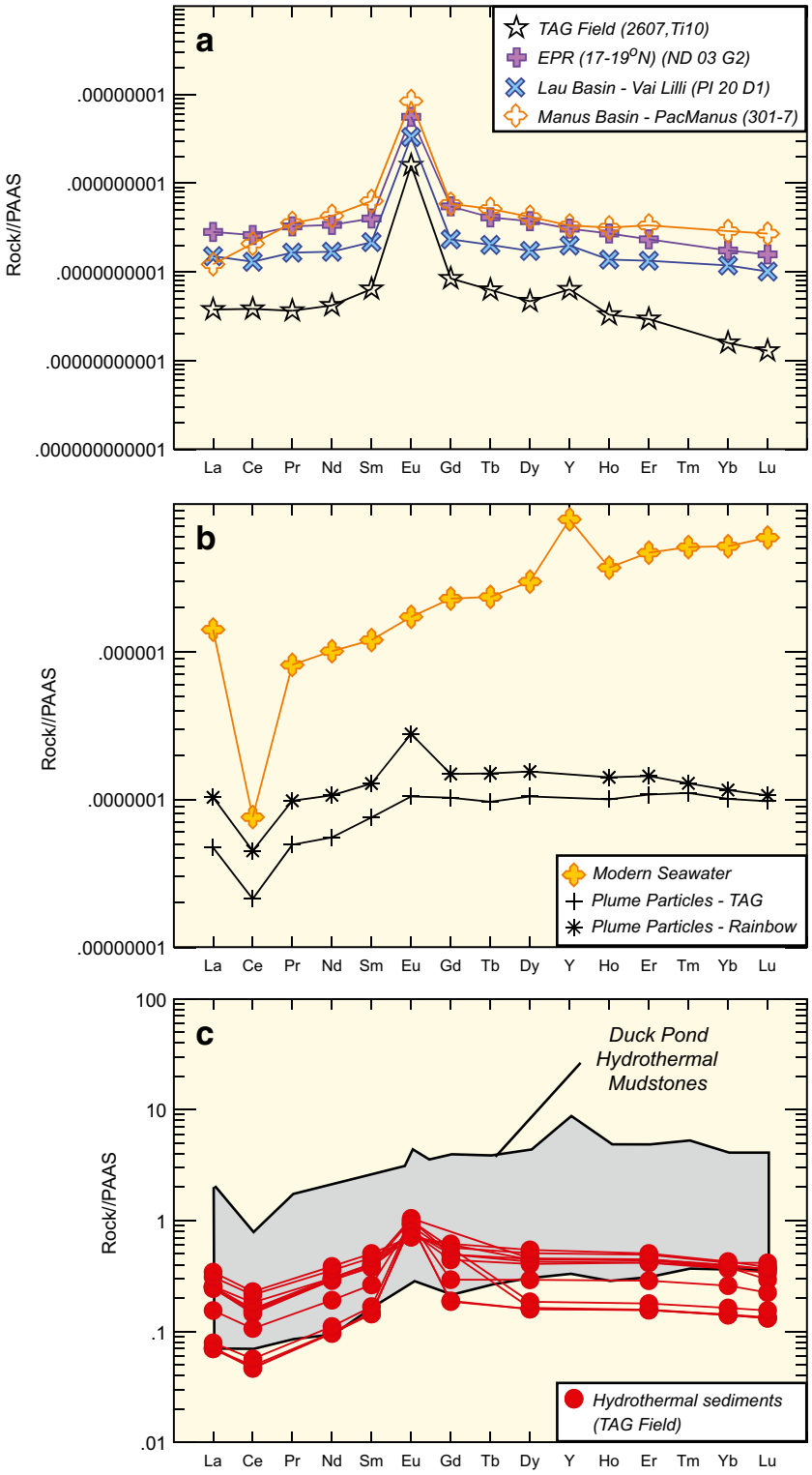

Fig. 13 Post-Archean Australian Shale (PAAS)-normalized REE-Y plots of modern vent fluids, particulates, seawater, and hydrothermal sedimentary rocks. **a** High temperature vent fluids from various vent fields, including TAG, East Pacific Rise (EPR), Vai Lilli, and PacManus (from Douville et al. 1999). **b** Modern seawater (Alibo and Nozaki 1999) and Fe-oxide/Fe-oxyhydroxide plume particles from the TAG (Sherrell et al. 1999) and Rainbow (Edmonds and German 2004) vent fields. **c** Modern hydrothermal sedimentary rocks derived from plume fallout from the TAG field (German et al. 1993). Shown for comparison is the field for the Duck Pond hydrothermal mudstones

rich mudstones. It is also possible that the enrichment in transition elements, like V and Ni, is due to detritus from the surrounding rocks, as some basaltic rocks have enrichments in these elements (Shervais 1982). This is inconsistent with the data for the mudstones, however, as they have V- and Ni-enrichments (i.e., V/V+Ni, Ni/Co) that are distinct from the bounding felsic and mafic rocks (Fig. 17), thus requiring an additional mechanism to explain their enrichment.

The enrichments in redox-sensitive elements such as V, Ni, and P, U, and Cd are most consistent with scavenging from seawater, similar to the interpretation for the REE-Y

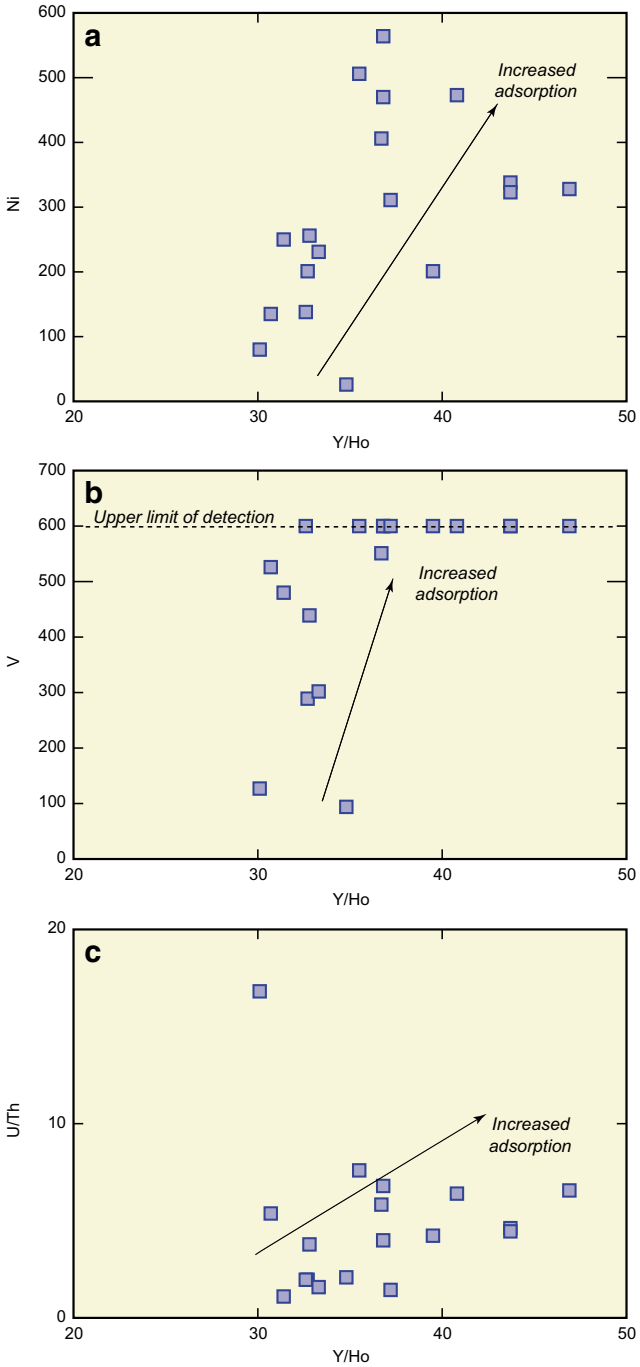

Fig. 15 Plots of Y/Ho versus redox-sensitive elements **a** Ni, **b** V, and **c** U/Th. These plots illustrate that these elements have been partly controlled by scavenging from oxygenated seawater

signatures (e.g., Figs. 12 and 15 and ESM Fig. 2). For example, numerous workers have illustrated that oxyanions like V, Ni, and U can be adsorbed onto Fe-oxide/oxyhydroxide particles in hydrothermal plumes (German et al. 1991a; Feely et al. 1998; German and von Damm 2003). Adsorption of oxyanions by Fe-oxide/oxyhydroxide particles is also supported by the correlation of V, Ni, U, P, and Cd with Y/Ho (Fig. 15 and ESM Fig. 2). Further, the negative correlation of P, U, Cd, V, and Ni with Ce/Ce* (ESM Figs. 2 and 3) illustrates that the highest concentrations of elements indicative of anoxic conditions are associated with the most negative Ce/Ce* values and the greatest indicator of oxygenated bottom waters, arguing that not only are these high concentrations in the Duck Pond hydrothermal mudstones indicative of scavenging, but also scavenging from oxygenated mid-Cambrian seawater. Support for venting into an oxygenated ocean is also corroborated by regional geology and stratigraphic relationships at the Lemarchant deposit, including the presence of bioturbation, open-system sulfur isotope fractionation, oxygen-rich seawater-like REE-Y systematics in correlative hydrothermal muds (Lode et al. 2016a, b), and hydrothermal barite that is intercalated with the mudstones that have textural and sulfur isotopic features indicative of venting into oxygenated seawater (Lajoie 2017).

The Duck Pond upper block hydrothermal mudstones formed from low-temperature (< 250 °C) fluids that vented into oxygenated mid-Cambrian seawater have minor detrital components, with the majority of their REE-Y and oxyanion budget controlled by scavenging from seawater by upwelling hydrothermal particles. These results also illustrate that some redox-sensitive trace elements (e.g., V, Ni, Co, U) must be used with caution for elucidating bottom water oxygen contents in basins that have evidence for hydrothermal activity.

Exploration implications

Understanding the relative contributions of hydrothermal vent-related elements versus oxidative scavenging from seawater is critical in utilizing hydrothermal mudstones as vectors to mineralization (Fig. 14; Peter 2003; Peter et al. 2003). The elevated base metal, Ba, S, and Fe_2O_3 contents, and Fe/Al and Fe-Al-Mn systematics of the Duck Pond hydrothermal sediments are indicative of a hydrothermal origin, consistent with the formation by venting of Fe-rich fluids onto the sea floor (Fig. 14; Peter 2003; Grenne and Slack 2005; Slack et al. 2009; Lode et al. 2015, 2016a, b). These results have important implications for exploration in the immediate Duck Pond area as the upper block has long been considered less prospective for VMS than the ore-hosting mineralized block. The hydrothermal mudstones have negative Eu anomalies on PAAS-normalized plots and Eu/Eu* ~ 1, however, indicating deposition from lower-temperature fluids (Sverjensky 1984); therefore, potential targets within the upper block and correlatives will likely be Zn-Pb-rich due to the temperature of hydrothermal venting (e.g., Lydon 1988; Large 1992). The Lemarchant deposit, which is 10 km along strike from the Duck Pond deposit (Fig. 2) and is hosted in similar aged rocks (~ 513 Ma), has similar stratigraphy and hydrothermal

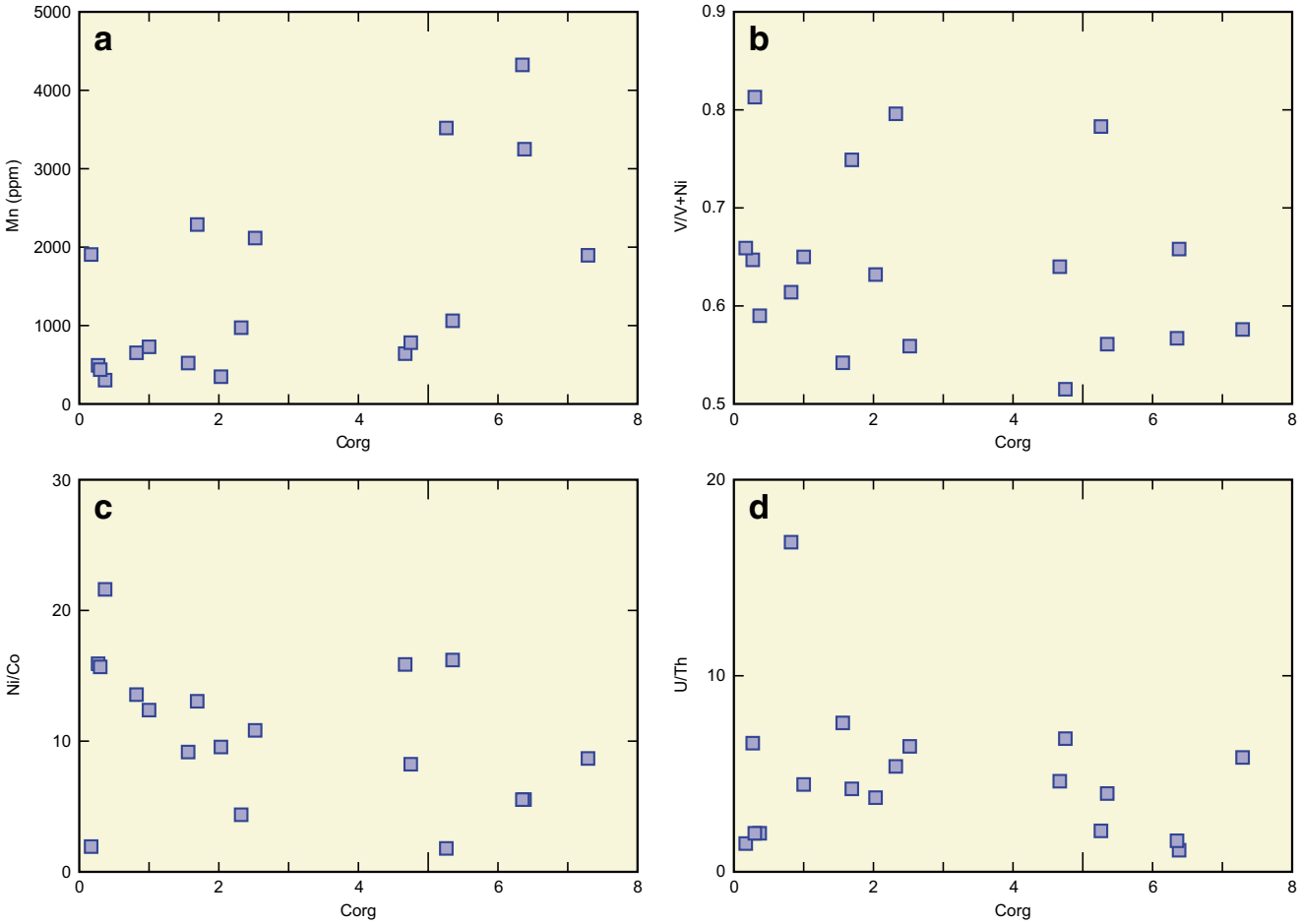

Fig. 16 Plots of C_{org} against key indicators of anoxic conditions in carbon-rich sedimentary rocks: **a** Mn, **b** V/V+Ni, **c** Ni/Co, and **d** U/Th. For details, see text

mudstones as the upper block at Duck Pond but the mudstones immediately overlie Zn-Pb-(Ba-Au-Ag)-rich VMS mineralization (Lode et al. 2015, 2016a, b; Cloutier et al. 2017; Gill et al. 2016). These regional stratigraphic and metallogenic correlations suggest that the Duck Pond upper block may have the potential to host Zn-Pb-(Ba-Au-Ag)-rich mineralization.

Despite the hydrothermal signatures in the Duck Pond upper block mudstones, they are likely vent-distal hydrothermal mudstones (Fig. 14), in contrast to the vent-proximal mudstones at Lemarchant (Lode et al. 2015, 2016a, b). The strong seawater REE-Y signatures (e.g., Ce/Ce* < 1, Y/Ho ~ 47) coupled with enrichment of adsorbed element enrichments suggest that the particles have had significant interaction with ambient seawater. Vented Fe-oxide/oxyhydroxide particles from buoyant plumes have considerable residence time in the ocean, often in excess of 50–60 days (Rudnicki 1995). Furthermore, particles can be found up to 10 km from the vent site with particles further away from the vent site often having greater REE-Y and oxyanion concentrations and more seawater-like signatures (Fig. 14) (German et al. 1990; Sherrell et al. 1999; German and Von Damm 2003). Therefore, given the strong seawater signature in the Duck Pond hydrothermal mudstones, it is entirely possible that they formed at distance from their vent sources, potentially as far as 10 km away (Fig. 14).

The results of this study are applicable to similar geological environments globally, as hydrothermal muds like those at Duck Pond are common in some ancient and modern VMS environments (Peter 2003), and they are potential vectors to mineralization. More prospective hydrothermal mudstones with the greatest potential should have elevated hydrothermal components (high Fe/Al, Zn, Cu, Hg, Hg/Na_2O, Ba, and Eu/Eu* > 1), with lesser to minor contributions from a detrital sedimentary material (e.g., Al_2O_3, Zr) and lesser to minor contributions of elements scavenged from seawater (Y/Ho ~ 27, low P_2O_5, U, Ni, Cr, V, Co).

Conclusions

Pyrite- and pyrrhotite-rich mudstones are common in rocks of the Tally Pond group and Victoria Lake supergroup,

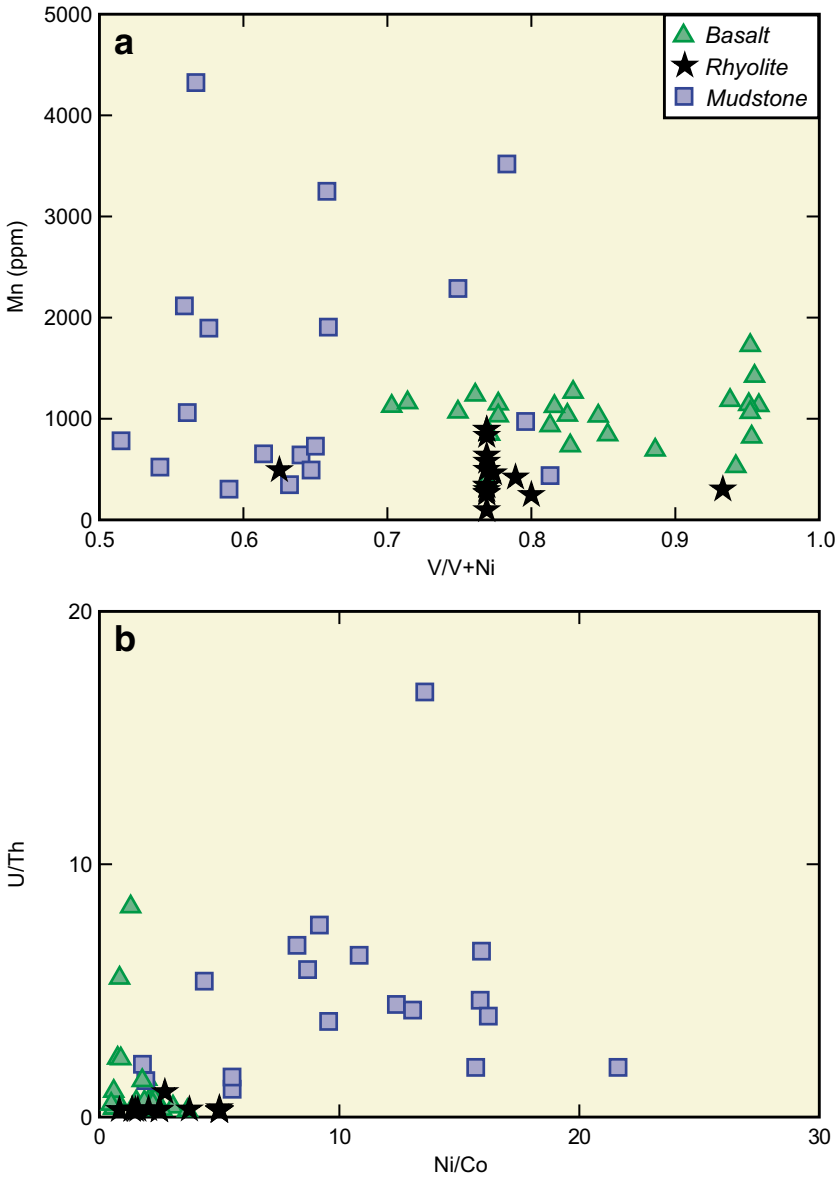

Fig. 17 Plots of redox-sensitive trace elements against one another and comparisons to potential detritus that may have controlled their distribution. **a** Mn-V/V+Ni. **b** Ni/Co-U/Th. The lack of overlap between the hydrothermal mudstones and the surrounding host rocks in the upper block suggests that the redox-sensitive elements and element ratios were not controlled by detritus from the basaltic and rhyolitic host rocks

central Newfoundland, Canada, and are spatially associated with volcanogenic massive sulfide (VMS) mineralization. The upper block of the Duck Pond deposit, despite being older than the main deposit and only weakly mineralized, contains abundant sulfide-rich mudstones. These mudstones are laminated, with variably carbon-rich layers alternating with sulfide-rich layers containing pyrrhotite and pyrite with lesser chalcopyrite, spalerite, galena, and arsenopyrite; based on textural evidence and isotopic data, these sulfides are interpreted to be predominantly diagenetic in origin with less input from hydrothermal fluids. The mudstone lithogeochemical signatures indicate a minor detrital component from rhyolite and basaltic host rocks, and a hydrothermal input recorded by the elevated Fe_2O_3 (~ 10–55%), S (~ 5–20), Pb (~ 20–100 ppm), Zn (~ 300–3000 ppm), Cu (~ 100–1000 ppm), and Ba (10–200 ppm) contents, and Fe/Al and Fe-Mn-Al systematics. The hydrothermal mudstones also contain enrichments in oxyanions such as P_2O_5, V, Cr, Ni, Co, and Cd that were likely derived from oxidative scavenging by Fe-oxide/oxyhydroxide particles from seawater. The REE-Y systematics of the hydrothermal mudstones corroborate oxidative scavenging by hydrothermal particles as the mudstones have signatures similar to modern oxygenated seawater with high Y/Ho and negative Ce anomalies (Ce/Ce* < 1), which are correlated with oxyanion concentrations; the samples also have low Eu/Eu* (i.e., ≤ 1). The collective lithogeochemical data point to the hydrothermal mudstones having formed from low-temperature (< 250 °C), Fe-rich hydrothermal vent fluids that likely formed a buoyant plume that vented into

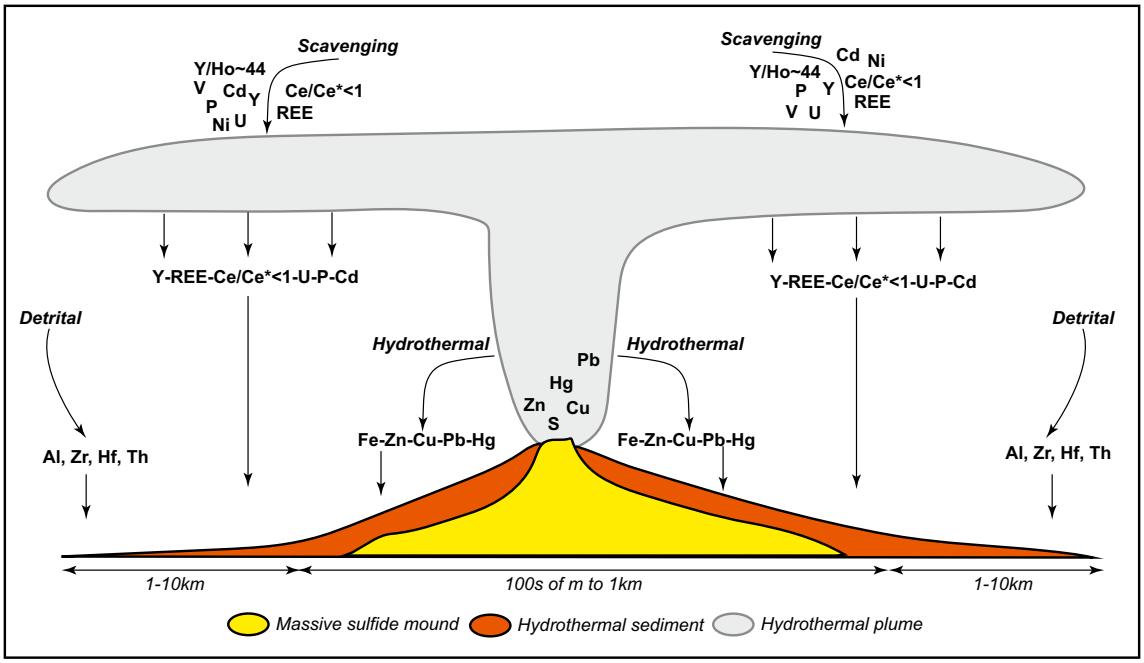

Fig. 14 Potential model for the geochemical systematics of the mudstones from the upper block of the Duck Pond deposit. Mudstones proximal to mineralization are dominated by hydrothermal components derived from upwelling hydrothermal fluids (base metals, Hg, Fe). With distance from the vent, there are greater contributions from detrital sedimentation (Al-Zr-Nb-Th) and components adsorbed from seawater (REE, Y, oxyanions). The estimates of distance are based on modern vent particle transport distances and knowledge from ancient hydrothermal sediments (Peter 2003). Diagram based on concepts outlined in Rudnicki (1995)

an oxygenated mid-Cambrian water column. The particles within the plume had sufficient residence time to scavenge elements and inherit a signature similar to ambient mid-Cambrian seawater.

The predominance of a seawater signature in most of the Duck Pond hydrothermal mudstones suggests that they are likely distal hydrothermal mudstones and, based on studies from modern hydrothermal plumes, could have been as far away as 10 km from their vent sources. Nevertheless, in vectoring within the Tally Pond belt, and similar belts globally, it is critical to find samples that have a hydrothermal signature (high Fe/Al, base metals, Ba, S), coupled with those that have a minimal seawater and adsorption signature (chondritic Y/Ho and Ce/Ce*, low P_2O_5, Ni, Co, Cr, V, Sb). Samples with hydrothermal signatures will indicate deposition in a near-vent environment with minimal residence time in the water column, and therefore potentially closer to mineralization.

Acknowledgements Numerous discussions with staff at the Duck Pond Mine, particularly Isobel Wolfson, Darren Hennessey, and Bernie Macneil, and ongoing discussions and collaborative research with John Hinchey of the Geological Survey of Newfoundland and Labrador on VMS deposits of central Newfoundland are gratefully acknowledged. Discussions with Balz Kamber, Jan Peter, and John Slack regarding the geochemical systematics of hydrothermal mudstones are greatly appreciated. Reviews of this manuscript by Craig Johnson, Jan Peter, Karen Kelley, and Georges Beaudoin have helped improve the manuscript and we thank them for their reviews and thoughtful comments.

Funding information This research project is part of the Canadian Mining Industry Research Organization (CAMIRO) Project 08E04 on the Geochemistry of Shales as Vectors to Ore Deposits funded by Actlabs, Barrick, Hudbay, Newmont, Selwyn Resources, Teck, Ur Energy, and an NSERC Collaborative Research and Development Grant (CRDPJ-387591-09). Initial financial and logistical support for this project was by research grants from Aur Resources Inc. (and subsequently Teck Resources Ltd.) and a Natural Sciences and Engineering Research Council of Canada (NSERC) Discovery Grant to Piercey. Piercey was also supported by the NSERC-Altius Industrial Research Chair in the Metallogeny of Ores in Volcanic and Sedimentary Basins at Memorial University supported by NSERC, Altius Resources Inc., and the Research and Development Corporation of Newfoundland and Labrador while this research was completed.

References

Alibo DS, Nozaki Y (1999) Rare earth elements in seawater; particle association, shale-normalization, and Ce oxidation. Geochim Cosmochim Acta 63(3-4):363–372. https://doi.org/10.1016/S0016-7037(98)00279-8

Bau M (1996) Controls on the fractionation of isovalent trace elements in magmatic and aqueous systems: evidence from Y/Ho, Zr/Hf, and lanthanide tetrad effect. Contrib Mineral Petrol 123(3):323–333. https://doi.org/10.1007/s004100050159

Bau M (1999) Scavenging of dissolved yttrium and rare earths by precipitating iron oxyhydroxide; experimental evidence for Ce oxidation,

Y-Ho fractionation, and lanthanide tetrad effect. Geochim Cosmochim Acta 63(1):67–77. https://doi.org/10.1016/S0016-7037(99)00014-9

Bau M, Koschinsky A, Dulski P, Hein JR (1996) Comparison of the partitioning behaviours of yttrium, rare earth elements, and titanium between hydrogenetic marine ferromanganese crusts and seawater. Geochim Cosmochim Acta 60(10):1709–1725. https://doi.org/10.1016/0016-7037(96)00063-4

Bau M, Moeller P, Dulski P (1997) Yttrium and lanthanides in eastern Mediterranean seawater and their fractionation during redox-cycling. Mar Chem 56(1-2):123–131. https://doi.org/10.1016/S0304-4203(96)00091-6

Bhatia MR, Crook KAW (1986) Trace element characteristics of graywackes and tectonic setting discrimination of sedimentary basins. Contrib Mineral Petrol 92(2):181–193. https://doi.org/10.1007/BF00375292

Boström K (1973) The origin and fate of ferromanganoan active ridge sediments. Stockh Contrib Geol 27:147–243

Boström K, Peterson MNA (1969) The origin of aluminum-poor ferromanganoan sediments in areas of high heat flow on the East Pacific Rise. Mar Geol 7(5):427–447. https://doi.org/10.1016/0025-3227(69)90016-4

Boström K, Joensuu O, Valdés S, Riera M (1972) Geochemical history of South Atlantic Ocean sediments since Late Cretaceous. Mar Geol 12(2):85–121. https://doi.org/10.1016/0025-3227(72)90023-0

Burnham OM, Schweyer J (2004) 54. Trace element analysis of geological samples by inductively coupled plasma mass spectrometry at the geoscience laboratories: revised capabilities due to improvements to instrumentation summary of fieldwork and other activities 2004. Ontario Geological Survey, pp 54.51–54.20

Calvert SE, Pedersen TF (1993) Geochemistry of recent oxic and anoxic marine sediments; implications for the geological record. Mar Geol 113(1-2):67–88. https://doi.org/10.1016/0025-3227(93)90150-T

Calvert SE, Pedersen TF (1996) Sedimentary geochemistry of manganese; implications for the environment of formation of manganiferous black shales. Econ Geol 91(1):36–47. https://doi.org/10.2113/gsecongeo.91.1.36

Chavagnac V, German CR, Milton JA, Palmer MR (2005) Sources of REE in sediment cores from the Rainbow vent site (36°14′N, MAR). Chem Geol 216(3-4):329–352. https://doi.org/10.1016/j.chemgeo.2004.11.015

Cloutier J, Piercey SJ, Lode S, Vande Guchte M, Copeland DA (2017) Lithostratigraphic and structural reconstruction of the Zn-Pb-Cu-Ag-Au Lemarchant volcanogenic massive sulphide (VMS) deposit, Tally Pond group, central Newfoundland, Canada. Ore Geol Revs 84:154–173. https://doi.org/10.1016/j.oregeorev.2017.01.010

de Baar HJW, German CR, Elderfield H, van Gaans P (1988) Rare earth element distributions in anoxic waters of the Cariaco Trench. Geochim Cosmochim Acta 52(5):1203–1219. https://doi.org/10.1016/0016-7037(88)90275-X

de Baar HJW, Schijf J, Byrne RH (1991) Solution chemistry of the rare earth elements in seawater. Eur J Solid State Inorg Chem 28:357–373

DeWolfe YM, Gibson HL, Piercey SJ (2009) Petrogenesis of the 1.9 Ga mafic hanging wall sequence to the Flin Flon, Callinan, and Triple 7 massive sulphide deposits, Flin Flon, Manitoba, Canada. Can J Earth Sci 46:509–527

Douville E, Bienvenu P, Charlou JL, Donval JP, Fouquet Y, Appriou P, Gamo T (1999) Yttrium and rare earth elements in fluids from various deep-sea hydrothermal systems. Geochim Cosmochim Acta 63(5):627–643. https://doi.org/10.1016/S0016-7037(99)00024-1

Dunning GR, Krogh TE (1985) Geochronology of ophiolites of the Newfoundland Appalachians. Can J Earth Sci 22(11):1659–1670. https://doi.org/10.1139/e85-174

Dunning GR, Kean BF, Thurlow JG, Swinden HS (1987) Geochronology of the Buchans, Roberts Arm, and Victoria Lake groups and Mansfield Cove Complex, Newfoundland. Can J Earth Sci 24(6):1175–1184. https://doi.org/10.1139/e87-113

Dunning GR, Swinden HS, Kean BF, Evans DTW, Jenner GA (1991) A Cambrian island arc in Iapetus: geochronology and geochemistry of the Lake Ambrose volcanic belt, Newfoundland Appalachians. Geol Mag 128(01):1–17. https://doi.org/10.1017/S0016756800018008

Edmonds HN, German CR (2004) Particle geochemistry in the Rainbow hydrothermal plume, Mid-Atlantic Ridge. Geochim Cosmochim Acta 68(4):759–772. https://doi.org/10.1016/S0016-7037(03)00498-8

Elderfield H, Greaves MJ (1982) The rare earth elements in seawater. Nature 296(5854):214–219. https://doi.org/10.1038/296214a0

Elderfield H, Charnock H, Lovelock JE, Liss PS, Whitfield M (1988) The oceanic chemistry of the rare-earth elements. Philos Trans R Soc Lond (Ser A) 325(1583):105–124. https://doi.org/10.1098/rsta.1988.0046

Eldridge CW, Barton PB, Ohmoto H (1983) Mineral textures and their bearing on formation of the Kuroko orebodies. Econ Geol Monogr 5:241–281

Evans DTW, Kean BF (1991) Metallogenic framework of base and precious metal deposits, central and western Newfoundland (Field Trip 1) Open-File Report-Geological Survey of Canada Report: 2156 pp. 46–55 1991

Evans DTW, Kean BF (2002) The Victoria Lake Supergroup, central Newfoundland—its definition, setting and volcanogenic massive sulphide mineralization Newfoundland and Labroador Department of Mines and Energy, Geological Survey, Open File NFLD/2790, pp 68

Evans DTW, Kean BF, Dunning GR (1990) Geological studies, Victoria Lake Group, Central Newfoundland. Curr Res Rep Geol Surv Branch Rep 90-1:131–144

Feely RA, Trefry JH, Massoth GJ, Metz S (1991) A comparison of the scavenging of phosphorus and arsenic from seawater by hydrothermal iron oxyhydroxides in the Atlantic and Pacific Oceans. Deep Sea Res Part A Ocean Res Paps 38(6):617–623. https://doi.org/10.1016/0198-0149(91)90001-V

Feely RA, Trefry JH, Lebon GT, German CR (1998) The relationship between P/Fe and V/Fe ratios in hydrothermal precipitates and dissolved phosphate in seawater. Geophys Res Lett 25(13):2253–2256. https://doi.org/10.1029/98GL01546

German CR, Von Damm KL (2003) Hydrothermal processes Treatise on Geochemistry Pergamon, pp 181–222. https://doi.org/10.1016/B0-08-043751-6/06109-0

German CR, Klinkhammer GP, Edmond JM, Mitra A, Elderfield H (1990) Hydrothermal scavenging of rare earth elements in the ocean. Nature 316:516–518

German CR, Campbell AC, Edmond JM (1991a) Hydrothermal scavenging at the Mid-Atlantic Ridge: modification of trace element dissolved fluxes. EPSL 107(1):101–114. https://doi.org/10.1016/0012-821X(91)90047-L

German CR, Holliday BP, Elderfield H (1991b) Redox cycling of rare earth elements in the suboxic zone of the Black Sea. Geochim Cosmochim Acta 55(12):3553–3558. https://doi.org/10.1016/0016-7037(91)90055-A

German CR, Higgs NC, Thomson J, Mills R, Elderfield H, Blusztajn J, Fleer AP, Bacon MP (1993) A geochemical study of metalliferous sediment from the TAG Hydrothermal Mound, 26°08'N, Mid-Atlantic Ridge. J Geophys Res 98(B6):9683–9692. https://doi.org/10.1029/92JB01705

Gill SB, Piercey SJ, Layton-Matthews D (2016) Mineralogy and metal zoning of the Lemarchant Zn-Pb-Cu-Au-Ag volcanogenic massive sulfide (VMS) deposit, Newfoundland. Can Mineral 54(5):1307–1344. https://doi.org/10.3749/canmin.1500069

Goodfellow WD, McCutcheon SR, Peter JM (eds) (2003a) Massive sulfide deposits of the Bathurst Mining Camp, New Brunswick, and Northern Maine. Society of Economic Geologists, Littleton, p 930

Goodfellow WD, Peter JM, Winchester JA, van Staal CR (2003b) Ambient marine environment and sediment provenance during formation of massive sulfide deposits in the Bathurst Mining Camp: importance of reduced bottom waters to sulfide precipitation and preservation. Econ Geol Monogr 11:129–156

Grenne T, Slack JF (2005) Geochemistry of jasper beds from the Ordovician Lokken Ophiolite, Norway; origin of proximal and distal siliceous exhalites. Econ Geol 100(8):1511–1527. https://doi.org/10.2113/gsecongeo.100.8.1511

Hibbard JP, van Staal CR, Rankin D, Williams H (2006) Lithotectonic map of the Appalachian Orogen, Canada–United States of America Geological Survey of Canada, pp Map 2096A, 1:1,500,000 scale

Hinchey JG (2007) Volcanogenic massive sulphides of the southern Tulks Volcanic Belt, central Newfoundland: Preliminary findings and overview of styles and environments of mineralization In Current Research. Geological Survey of Newfoundland and Labrador, St. John's, NL, Canada, pp 117–143

Hinchey JG (2008) Volcanogenic massive sulfides of the northern Tulks Volcanic Belt, central Newfoundland: preliminary findings, overview of deposit reclassifications, and mineralizing environments. In Current research. Geological Survey of Newfoundland and Labrador, St. John's, NL, Canada pp 151–172

Hinchey JG (2011) The Tulks Volcanic Belt, Victoria Lake Supergroup, Central Newfoundland—geology, tectonic setting, and volcanogenic massive sulfide mineralization Geological Survey of Newfoundland and Labrador, St. John's, NL, Canada, Report 2011-02, pp 167

Hinchey JG (2014) The Long Lake Group: preliminary U-Pb geochronology and lithogeochemistry, and implications for tectonostratigraphic architecture and VMS mineralization. In Current research. Geological Survey of Newfoundland and Labrador, St. John's, NL, Canada pp. 15–44

Hinchey JG, McNicoll V (2009) Tectonostratigraphic architecture and VMS mineralization of the southern Tulks Volcanic Belt: new insights from U-Pb geochronology and lithogeochemistry In Current Research. Geological Survey of Newfoundland and Labrador, St. John's, NL, Canada, pp 13–42

Hrischeva E, Scott SD (2007) Geochemistry and morphology of metalliferous sediments and oxyhydroxides from the Endeavour segment, Juan de Fuca Ridge. Geochim Cosmochim Acta 71(14):3476–3497. https://doi.org/10.1016/j.gca.2007.03.024

Hrischeva E, Scott SD, Weston R (2007) Metalliferous sediments associated with presently forming volcanogenic massive sulfides: the SuSu Knolls Hydrothermal Field, Eastern Manus Basin, Papua New Guinea. Econ Geol 102(1):55–73. https://doi.org/10.2113/gsecongeo.102.1.55

Jenner GA, Dunning GR, Malpas J, Brown M, Brace T (1991) Bay of Islands and Little Port complexes, revisited; age, geochemical and isotopic evidence confirm suprasubduction-zone origin. Can J Earth Sci 28(10):1635–1652. https://doi.org/10.1139/e91-146

Jones B, Manning DAC (1994) Comparison of geochemical indices used for the interpretation of palaeoredox conditions in ancient mudstones. Chem Geol 111(1-4):111–129. https://doi.org/10.1016/0009-2541(94)90085-X

Kalogeropoulos SI, Scott SD (1983) Mineralogy and geochemistry of tuffaceous exhalites (Tetsusekiei) of the Fukazawa mine, Hokuroko District, Japan. Econ Geol Monogr 5:412–432

Kalogeropoulos SI, Scott SD (1989) Mineralogy and geochemistry of an Archean tuffaceous exhalite; the Main Contact Tuff, Millenbach Mine area, Noranda, Quebec. Can J Earth Sci 26(1):88–105. https://doi.org/10.1139/e89-008

Kamber BS, Webb GE (2001) The geochemistry of late Archaean microbial carbonate: implications for ocean chemistry and continental erosion history. Geochim Cosmochim Acta 65(15):2509–2525. https://doi.org/10.1016/S0016-7037(01)00613-5

Kamber BS, Bolhar R, Webb GE (2004) Geochemistry of late Archaean stromatolites from Zimbabwe: evidence for microbial life in restricted epicontinental seas. Precambrian Res 132(4):379–399. https://doi.org/10.1016/j.precamres.2004.03.006

Kean BF (1985) Metallogeny of the Tally Pond Volcanics, Victoria Lake Group, central Newfoundland. Report-Government of Newfoundland and Labrador, Department of Mines and Energy, Mineral Development Division 85-1:89–93

Kean BF, Evans DTW (1986) Metallogeny of the Tulks Hill Volcanics, Victoria Lake Group, central Newfoundland. In Current research. Geological Survey of Newfoundland and Labrador, St. John's, NL, Canada., 51–57

Kean BF, Evans DTW, Jenner GA (1995) Geology and mineralization of the Lushs Bight Group. Geological Survey of Newfoundland and Labrador, St. John's, NL, Canada, Report 1995–2, pp 204

Lajoie M-E (2017) Genesis of barite associated with the Lemarchant Zn-Pb-Cu-Ag-Au-rich volcanogenic massive sulfide (VMS) deposit: implications for the genesis of VMS-related barite, Cambrian seawater chemistry, and the origin of barite-rich VMS dpeosits. Unpublishd MSc thesis, Memorial University of Newfoundland, St. John's, Canada, pp 300

Large RR (1992) Australian volcanic-hosted massive sulfide deposits; features, styles, and genetic models. Econ Geol 87(3):471–510. https://doi.org/10.2113/gsecongeo.87.3.471

Lode S, Piercey SJ, Devine CA (2015) Geology, mineralogy, and lithogeochemistry of metalliferous mudstones associated with the Lemarchant volcanogenic massive sulfide deposit, Tally Pond Belt, Central Newfoundland. Econ Geol 110(7):1835–1859. https://doi.org/10.2113/econgeo.110.7.1835

Lode S, Piercey SJ, Layne GD, Piercey G, Cloutier J (2016a) Multiple sulphur and lead sources recorded in hydrothermal exhalites associated with the Lemarchant volcanogenic massive sulphide deposit, central Newfoundland, Canada. Mineral Deposita

Lode S, Piercey SJ, Squires GC (2016b) Role of metalliferous mudstones and detrital shales in the localization, genesis, and paleoenvironment of volcanogenic massive sulphide deposits of the Tally Pond volcanic belt, central Newfoundland, Canada. Can J Earth Sci 53(4):387–425. https://doi.org/10.1139/cjes-2015-0155

Lydon JW (1988) Volcanogenic massive sulphide deposits; Part 2, Genetic models. Geosci Can 15:43–65

MacDonald PJ, Piercey SJ, Hamilton MA (2005) Discover Abitibi Intrusion Subproject: an integrated study of intrusive rocks spatially associated with gold and base metal mineralization in Abitibi greenstone belt, Timmins area and Clifford township. Ontario Geological Survey, Sudbury

MacLachlan K, Dunning G (1998a) U-Pb ages and tectono-magmatic evolution of Middle Ordovician volcanic rocks of the Wild Bight Group, Newfoundland Appalachians. Can J Earth Sci 35(9):998–1017. https://doi.org/10.1139/e98-050

MacLachlan K, Dunning GR (1998b) U-Pb ages and tectonomagmatic relationships to early Ordovician low-Ti tholeiites, boninites, and related plutonic rocks in central Newfoundland, Canada. Contrib Mineral Petrol 133(3):235–258. https://doi.org/10.1007/s004100050450

MacLean WH (1990) Mass change calculations in altered rock series. Mineral Deposita 25(1):44–49. https://doi.org/10.1007/BF03326382

McLennan SM (2001) Relationships between the trace element composition of sedimentary rocks and upper continental crust. G-cubed 2: 24 (Paper 2000GC000109)

McLennan SM, Hemming S, McDaniel DK, Hanson GN (1993) Geochemical approaches to sedimentation, provenance, and tectonics. Spec Pap Geol Soc Am 284:21–40. https://doi.org/10.1130/SPE284-p21

McLennan SM, Bock B, Hemming SR, Hurowitz JA, Lev SM, McDaniel DK (2003) The roles of provenance and sedimentary processes in

the geochemistry of sedimentary rocks. In: Lentz DR (ed) Geochemistry of sediments and sedimentary rocks: evolutionary considerations to mineral deposit-forming environments. Geological Association of Canada, St. John's, pp 7–38

McNicoll V, Squires G, Kerr A, Moore P (2010) The Duck Pond and Boundary Cu-Zn deposits, Newfoundland: new insights into the ages of host rocks and the timing of VHMS mineralization. Can J Earth Sci 47(12):1481–1506. https://doi.org/10.1139/E10-075

Michard A (1989) Rare earth element systematics in hydrothermal fluids. Geochim Cosmochim Acta 53(3):745–750. https://doi.org/10.1016/0016-7037(89)90017-3

Michard A, Albarede F, Michard G, Minster JF, Charlou JL (1983) Rare-earth elements and uranium in high-temperature solutions from East Pacific Rise hydrothermal vent field (13 degrees N). Nature 303(5920):795–797. https://doi.org/10.1038/303795a0

Mills RA (1995) Hydrothermal activity and the geochemistry of metalliferous sediment. AGU Geophys Monogr 91:392–407

Mitra A, Elderfield H, Greaves MJ (1994) Rare earth elements in submarine hydrothermal fluids and plumes from the Mid-Atlantic Ridge. Mar Chem 46(3):217–235. https://doi.org/10.1016/0304-4203(94)90079-5

Moore PJ (2003) Stratigraphic implications for mineralization; preliminary findings of a metallogenic investigation of the Tally Pond Volcanics, central Newfoundland. In Current research. Geological Survey of Newfoundland and Labrador, St. John's, NL, Canada, pp 241–257

Nesbitt HW (2003) Petrogenesis of siliciclastic sediments and sedimentary rocks In: Lentz DR (ed) Geochemistry of sediments and sedimentary rocks: evolutionary considerations to mineral deposit-forming environments. Geological Association of Canada, St. John's, NL, Canada, pp 39–52

Nesbitt HW, Young GM (1984) Prediction of some weathering trends of plutonic and volcanic rocks based on thermodynamic and kinetic considerations. Geochim Cosmochim Acta 48(7):1523–1534. https://doi.org/10.1016/0016-7037(84)90408-3

Nozaki Y, Zhang J, Amakawa H (1997) The fractionation between Y and Ho in the marine environment. Earth and Planetary Science Letters 148:329-340

Nozaki Y, Alibo DS (2003) Importance of vertical geochemical processes in controlling the oceanic profiles of dissolved rare earth elements in the northeastern Indian Ocean. EPSL 148:329–340

Peter JM (2003) Ancient iron formations: their genesis and use in the exploration for stratiform base metal sulphide deposits, with examples from the Bathurst Mining Camp In: Lentz DR (ed) Geochemistry of sediments and sedimentary rocks: secular evolutionary considerations to mineral deposit-forming environments. Geological Association of Canada, pp 145–176

Peter JM, Goodfellow WD (1996) Mineralogy, bulk and rare earth element geochemistry of massive sulphide-associated hydrothermal sediments of the Brunswick Horizon, Bathurst Mining Camp, New Brunswick. Can J Earth Sci 33(2):252–283. https://doi.org/10.1139/e96-021

Peter JM, Goodfellow WD, Doherty W (2003) Hydrothermal sedimentary rocks of the Heath Steele belt, Bathurst mining camp, New Brunswick: part 2. Bulk and rare earth element geochemistry and implications for origin. Econ Geol Monogr 11:391–415

Piercey SJ (2007a) Summary report for Aur resources: Duck Pond site visit, July 30 to August 10th, 2007, Internal Report, Aur Resources pp 9

Piercey SJ (2007b) Summary report for Aur resources: Duck Pond site visit, June 18-29th, 2007, pp 11

Piercey SJ (2007c) Volcanogenic massive sulphide (VMS) deposits of the Newfoundland Appalachians: an overview of their setting, classification, grade-tonnage data, and unresolved questions In Current Research. Geological Survey of Newfoundland and Labrador, St. John's, NL, Canada, pp 169–178

Piercey SJ, Layne GD, Piercey G, Squires GC, Brace TD (2013) Geology, lithogeochemistry, and sulfur isotope geochemistry of hydrothermal mudstones from the Duck Pond volcanogenic massive sulfide (VMS) deposit, Newfoundland Appalachians, Canada Mineral Deposits Research for a High-Tech World: 12th SGA Biennial Meeting. Uppsala, Sweden, pp 572–575

Piercey SJ, Squires GC, Brace TD (2014) Lithostratigraphic, hydrothermal, and tectonic setting of the boundary volcanogenic massive sulfide deposit, Newfoundland Appalachians, Canada: formation by subseafloor replacement in a Cambrian rifted arc. Econ Geol 109(3):661–687. https://doi.org/10.2113/econgeo.109.3.661

Pollock J (2004) Geology and paletectonic history of the Tally Pond Group, Dunnage Zone, Newfoundland Appalachians: an integrated geochemical, geochronological, metallogenic and isotopic study of a Cambrian island arc along the peri-Gondwanan margin of Iapetus. Unpublished MSc thesis, Memorial University of Newfoundland, St. John's, Canada, pp 420

Quinby-Hunt MS, Wilde P (1994) Thermodynamic zonation in the black shale facies based on iron-manganese-vanadium content. Chem Geol 113:3–4

Rogers N, van Staal CR (2002) Toward a Victoria Lake Supergroup: a provisional stratigraphic revision of the Red Indian to Victoria lakes area, central Newfoundland. In Current research. Geological Survey of Newfoundland and Labrador, St. John's, NL, Canada,, pp 185–195

Rogers N, van Staal CR, McNicoll V, Pollock J, Zagorevski A, Whalen J (2006) Neoproterozoic and Cambrian arc magmatism along the eastern margin of the Victoria Lake Supergroup: a remnant of Ganderian basement in central Newfoundland? Precambrian Res 147(3-4):320–341. https://doi.org/10.1016/j.precamres.2006.01.025

Rogers N, van Staal C, Zagorevski A, Skulski T, Piercey SJ, McNicoll V (2007) Timing and tectonic setting of volcanogenic massive sulphide bearing terranes within the Central Mobile Belt of the Canadian Appalachians In: Milkereit B (ed) Proceedings of Exploration 07: Fifth Decennial International Conference on Mineral Exploration. Toronto, ON, pp 1199–1205

Rudnicki MD (1995) Particle formation, fallout and cycling within the buoyant and non-buoyant plume above the TAG vent field. Geol Soc Lond Spec Pub 87(1):387–396. https://doi.org/10.1144/GSL.SP.1995.087.01.30

Ruks TW, Piercey SJ, Ryan JJ, Villeneuve ME, Creaser RA (2006) Mid- to late Paleozoic K-feldspar augen granitoids of the Yukon-Tanana terrane, Yukon, Canada: implications for crustal growth and tectonic evolution of the northern Cordillera. Geol Soc Am Bull 118(9-10):1212–1231. https://doi.org/10.1130/B25854.1

Sherrell RM, Field MP, Ravizza G (1999) Uptake and fractionation of rare earth elements on hydrothermal plume particles at 9°45′N, East Pacific Rise. Geochim Cosmochim Acta 63(11-12):1709–1722. https://doi.org/10.1016/S0016-7037(99)00182-9

Shervais JW (1982) Ti-V plots and the petrogenesis of modern and ophiolitic lavas. EPSL 59(1):101–118. https://doi.org/10.1016/0012-821X(82)90120-0

Skulski T, Castonguay S, McNicoll VJ, van Staal C (2008) New constraints on the geology of Baie Berte Peninsula, Newfoundland; part 1, Tectonostratigraphy of ophiolites and their volcanic cover Abstracts with Programs-Geological Society of America. Boulder, CO, United States, United States, pp 28–28

Skulski T, Castonguay S, McNicoll V, van Staal C, Kidd W, Rogers N, Morris W, Ugalde H, Slavinski H, Spicer W, Moussallam Y, Kerr I (2010) Tectonostratigraphy of the Baie Verte oceanic tract and its ophiolite cover sequence on the Baie Verte Peninsula. In Current research. Geological Survey of Newfoundland and Labrador, St. John's, NL, Canada, pp 315–225

Slack JF, Grenne T, Bekker A, Rouxel OJ, Lindberg PA (2007) Suboxic deep seawater in the late Paleoproterozoic: evidence from hematitic chert and iron formation related to seafloor-hydrothermal sulfide

deposits, central Arizona, USA. EPSL 255(1-2):243–256. https://doi.org/10.1016/j.epsl.2006.12.018

Slack JF, Grenne T, Bekker A (2009) Seafloor-hydrothermal Si-Fe-Mn exhalites in the Pecos greenstone belt, New Mexico, and the redox state of ca. 1720 Ma deep seawater. Geosphere 5(3):302–314. https://doi.org/10.1130/GES00220.1

Squires GC, Moore PJ (2004) Volcanogenic massive sulphide environments of the Tally Pond Volcanics and adjacent area; geological, lithogeochemical and geochronological results In Current Research. Geological Survey of Newfoundland and Labrador, St. John's, NL, Canada, pp 63–91

Squires GC, MacKenzie AC, MacInnis D (1991) Geology and genesis of the Duck Pond volcanogenic massive sulfide deposit. In: Swinden HS, DTW E, Kean BF (eds) Metallogenic framework of base and precious metal deposits, central and western Newfoundland. Geological Survey of Canada, Ottawa, pp 56–64

Squires GC, Brace TD, Hussey AM (2001) Newfoundland's polymetallic Duck Pond deposit: earliest Iapetan VMS mineralization formed within a sub-seafloor, carbonate-rich alteration system. In: DTW E, Kerr A (eds) Geology and Mineral Deposits of the Northern Dunnage Zone, Newfoundland Appalachians. Geological Association of Canada/Mineralogical Association of Canada, St. John's, pp 167–187

Sverjensky DA (1984) Europium redox equilibria in aqueous solutions. EPSL 67(1):70–78. https://doi.org/10.1016/0012-821X(84)90039-6

Swinden HS (1991) Paleotectonic settings of volcanogenic massive sulphide deposits in the Dunnage Zone, Newfoundland Appalachians. CIM Bull 84:59–89

Swinden HS, Jenner GA, Kean BF, Evans DTW (1989) Volcanic rock geochemistry as a guide for massive sulphide exploration in central Newfoundland In Current Research. Geological Survey of Newfoundland and Labrador, St. John's, NL, Canada, pp 201–219

Thurlow JG (2010) Great mining camps of Canada 3. The history and geology of the Buchans mine, Newfoundland and Labrador. Geosci Can 37:145–173

Tribovillard N, Algeo TJ, Lyons T, Riboulleau A (2006) Trace metals as paleoredox and paleoproductivity proxies: an update. Chem Geol 232(1-2):12–32. https://doi.org/10.1016/j.chemgeo.2006.02.012

van Staal CR (2007) Pre-Carboniferous tectonic evolution and metallogeny of the Canadian Appalachians In: Goodfellow WD (ed) Mineral deposits of Canada: a synthesis of major deposit-types, district metallogeny, the evolution of geological provinces, and exploration methods. Special Publication 5, Mineral Deposits Division, Geological Association of Canada, pp 793–818

van Staal C, Barr SM (2012) Lithospheric architecture and tectonic evolution of the Canadian Appalachians and associated Atlantic margin. Chapter 2. In: Percival JA, Cook FA, Clowes RM (eds) In Tectonic styles in Canada: the LITHOPROBE perspective. Geological Association of Canada, St. John's, pp 41–96

van Staal CR, Colman-Sadd SP (1997) The central mobile belt of the northern Appalachians. Oxf Monogr Geol Geophys 35:747–760

Williams H (1979) Appalachian orogen in Canada. Can J Earth Sci 16(3): 792–807. https://doi.org/10.1139/e79-070

Williams H, Colman-Sadd SP, Swinden HS (1988) Tectonostratigraphic subdivisions of central Newfoundland. Current Research, Part B. Geological Survey of Canada, Ottawa, ON, Canada, pp 91–98

Zagorevski A, van Staal CR, McNicoll VJ (2007a) Distinct Taconic, Salinic, and Acadian deformation along the Iapetus suture zone, Newfoundland Appalachians. Can J Earth Sci 44(11):1567–1585. https://doi.org/10.1139/e07-037

Zagorevski A, van Staal CR, McNicoll VJ, Rogers N (2007b) Upper Cambrian to Upper Ordovician peri-Gondwanan island arc activity in the Victoria Lake Supergroup, central Newfoundland: tectonic development of the northern Ganderian margin. Am J Sci 307(2): 339–370. https://doi.org/10.2475/02.2007.02

Zagorevski A, van Staal CR, Rogers N, McNicoll VJ, Pollock J (2010) Middle Cambrian to Ordovician arc-backarc development on the leading edge of Ganderia, Newfoundland Appalachians. Geol Soc Am Mem 206:367–396. https://doi.org/10.1130/2010.1206(16)